Is Now Part of

ON Semiconductor®

To learn more about ON Semiconductor, please visit our website at
www.onsemi.com

Application Note AN9039

Using the FDMS2380 Dual Integrated Solenoid Driver

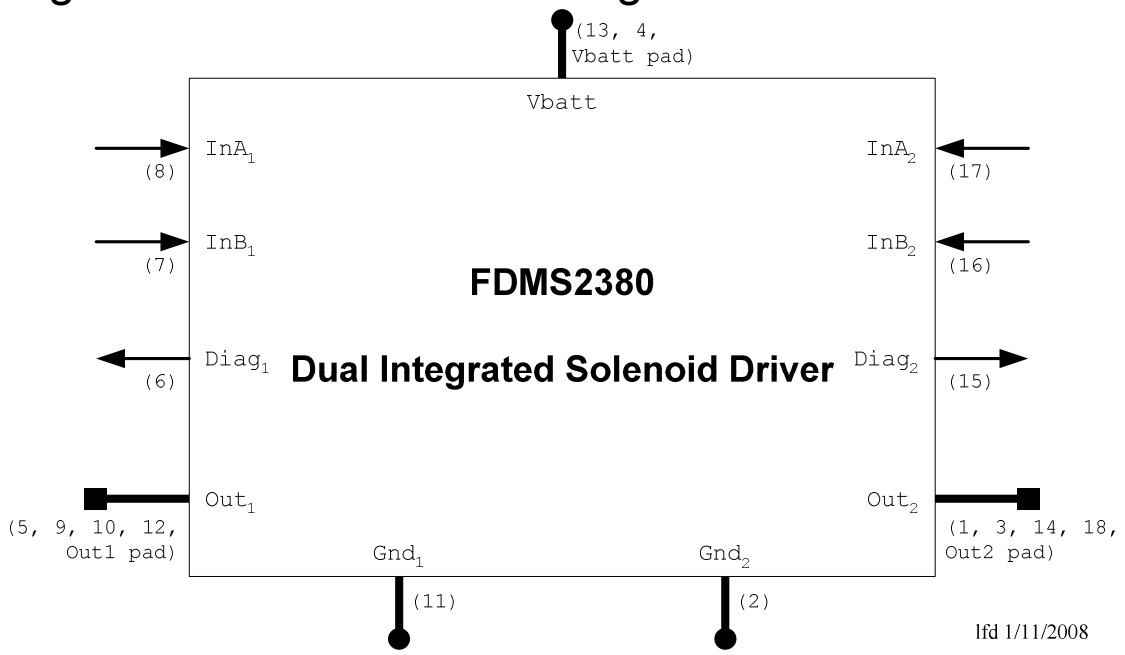

Figure 1: FDMS2380 I/O Block Diagram

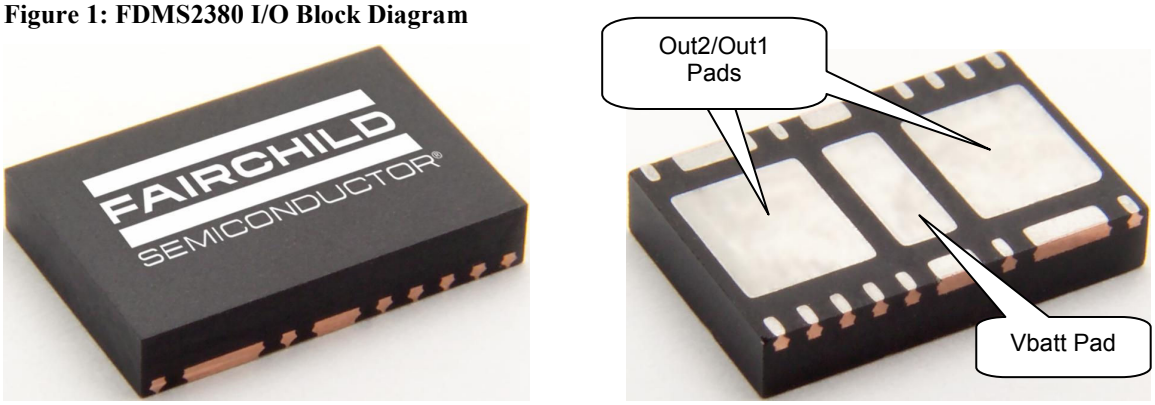

Figure 2: The FDMS2380 Power QFN Package

Table of Contents

Introduction

The FDMS2380 Dual Integrated Solenoid Driver product (also referred to as the DISD) is an integrated load management device specifically designed for driving inductive loads (the FDMS2380 package is shown in Figure 2). It contains two (2) electrically independent channels that not only control the load, but also provide fault detection logic and protection features. Although the FDMS2380 was designed with solenoids as the target application, any inductive device can be controlled with it.

Although it could be used in other configurations, the basic application diagram for the device is shown in Figure 42 on page 40.

It is highly recommended that the reader carefully review the FDMS2380 data sheet before reading this applications note. Some hands-on use of the device in a demonstration board, or in a test board would be helpful as well.

This application note covers a basic overview of solenoids, the FDMS2380 product, some applications for it, and design information aimed at simplifying the use of the device.

The appendix "*A.6: Definition of Terms and Symbols*" should be referenced regularly while reading this applications note to clarify the exact terminology and symbols used throughout. Furthermore, the other appendices are available to supply a more detailed analysis of shorter discussions in the main text.

Introduction to Solenoids

A solenoid is a fundamental device that converts electrical energy (the timed application of voltage and current) into mechanical energy (motion of a mass). Solenoids are used in many applications including automotive (e.g., automatic transmissions, injector valves, door locks, etc.), industrial (e.g., valve control, electromechanical access safety interlocks, vent activation, etc.) and many others. Typically, solenoids are used in a snap action fashion such that the device is electrically activated in one direction and when electrically deactivated, it returns to the initial position with the restoring force of a mechanical spring. There are however, applications for bidirectional actuation (e.g., with dual opposing coils etc.) and also linear controlled devices (i.e., servo controlled with position and/or force feedback). This application note will focus on linear solenoids, but the information applies to rotary solenoids as well. Furthermore, the focus will be on solenoids operated in a snap action fashion (i.e., not servo controlled), although the FDMS2380 would be useful in a servo mode too.

Basic Physics

A series of well known scientific principles involving current through conductors and the resultant magnetic forces that impinge on certain nearby objects are manipulated to form the device known as a solenoid.

First, when current flows through a conductor, a magnetic field appears around the conductor (Ampère's law, discovered by André-Marie Ampère, relates the circulating magnetic field in a closed loop to the electric

current passing through the loop). The magnitude of the current determines the intensity of the magnetic field and the current flow polarity determines the direction of the magnetic flux. In ordinary circumstances, the magnet field is oriented to apply a force to nearby ferromagnetic materials (e.g., cold rolled steel) to cause motion. The generated magnetic field follows the so-called right hand rule, whereby if the thumb of the right hand is pointed in the direction of the current flow, the fingers wrapping around the conductor will point in the direction of the magnet field.

Next, as changing magnetic flux crosses a conductor, a voltage is induced in the conductor (note that a static field, and no relative motion, induces no voltage). The changing magnetic flux can be produced by either a time-varying field or by physical motion between the field and the conductor.

Next, if the wire is made into a cylindrical spiral coil with N turns, the magnetic intensity from each turn is concentrated along the center-line axis of the cylinder. The magnetic flux density along the center axis becomes N times greater (the flux density varies along the length of the center axis with the ends being the lowest density).

The magnetic field can be further concentrated using a ferromagnetic core material inserted in the coil so as to be surrounded by the windings. A ferromagnetic material enclosing the coil will concentrate the field even more.

Two types of linear solenoid are the paddle (or flapper) type (see Figure 3) and the tubular type (see Figure 4).

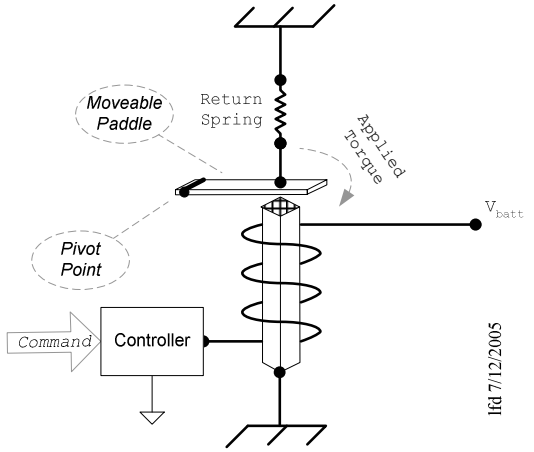

Figure 3: Paddle or Flapper Type Solenoid

The force applied to the paddle (Figure 3) is inversely proportional to two times the square of the distance between the core end and the paddle (this is highly dependant on the materials involved). The implication is that when current is first applied to the solenoid coil, the force is at its minimum over the total travel. However, as the paddle moves towards the coil, the force rapidly increases.

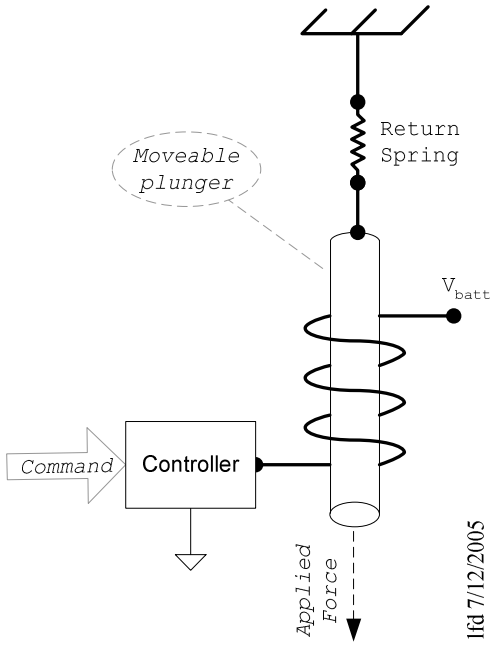

Figure 4: Tubular Solenoid

This means that the holding force to maintain the final position can require less current than the starting pull-in force. The tubular solenoid (Figure 4) acts in a similar fashion.

As current flows into the coil, energy is stored in the magnetic field. When the solenoid needs to be turned off, the energy stored in the magnetic field must be dissipated (often referred to as de-magnetization or de-energization) before the solenoid will disengage and return to its resting position. As the magnetic field collapses, a voltage is induced in the coil (back EMF) to an amount proportional to the coil inductance multiplied by the time rate of change of the electrical current and so the voltage across the solenoid will increase (sometimes referred to as flyback voltage). The magnitude of this voltage can be very high and must be accounted for in the design of control circuits. Furthermore, the energy dissipation to collapse the magnetic field can be large and must also be accounted for when using the FDMS2380 device (this will be covered in more detail later in this applications note).

In summary, the solenoid is activated initially with a large current to make sure that it moves the target mass to the engaged position (magnetic force can be inversely proportional to the square of the distance). Once the solenoid is in position, a smaller current is needed to maintain that position (smaller current means smaller power). When the solenoid is disengaged, the energy stored in the magnet field must be dissipated. The dissipation process produces high flyback voltages (a level proportional to the inductance times the time rate of change of the current) and the energy needs to be dissipated in the control device.

Governing Equations

Two key elements to the understanding of the operation of solenoids is the relationship between current flowing through the device and the associated voltage across it and the force produced by the current flowing through the coil. In the following two sections, mathematical models will be developed for each element to help in the understanding of solenoids.

Simple Mathematical Model

One model of a solenoid consists of an ideal inductor (whose inductance varies with position) in series with a resistor (whose value changes with temperature) as shown in Figure 5. It should be noted that other complexities including magnetic saturation of the core are not considered here.

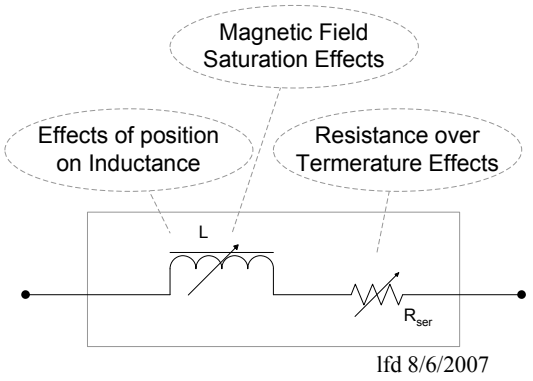

Figure 5: One Possible Model of a Solenoid

The nominal inductance of the solenoid is dependent on construction parameters including the geometry of the windings, the inside and outside diameter of the coils, the diameter of the wire, the wire material, the number of turns and the core material (i.e., various grades of steel, etc.). As the solenoid is activated and the motion element changes position with respect to the coil, the inductance will change. As an example, one particular paddle type solenoid that was evaluated in the lab had a measured inductance that varied by as much as 50% between the rest position (plunger out of the solenoid) and the activated position (plunger fully inserted).

The nominal resistance value of the coil is based on the resistance/length of the wire (given at a particular temperature) multiplied times the length of the wire. As current flows through the solenoid, heat is generated to elevate the wire temperature above ambient. This will increase the total D.C. resistance of the coil. The resistance of the copper wire in the coil can vary by nearly 2:1 when operated over the entire automotive temperature range (-40°C to +150°C)[1]. An example of this is shown in the following section.

[1] See section "*Practical Considerations*" on page 9 and the appendix "*A.1: Example Estimating Coil Wire Length and D. C. Resistance Change over Temperature*" on page 42 for more details.

The equation for the voltage across an ideal inductor is:

Equation 1: $V = L\frac{di}{dt}$

A simple inductive circuit (see Figure 6) that has an inductor (L), its internal resistance (R_{ser}), source resistance (R_{src}), a switch (S_1 activates and deactivates the solenoid) and a resistor (R_{off}) to help dissipate the energy in the solenoid when deactivating. Notice that this simplified model does not take into account changes in the resistance or inductance as described previously.

Using Kirchhoff's 2nd law for the case when S_1 is in the closed position (activating the solenoid), the circuit equation becomes:

Equation 2: $V_{batt} = i \times (R_{src} + R_{ser}) + L\frac{di}{dt}$

It is assumed here that the differential equation's initial condition is zero current flow in the circuit and that S_1 is ideal with no resistance or inductance.

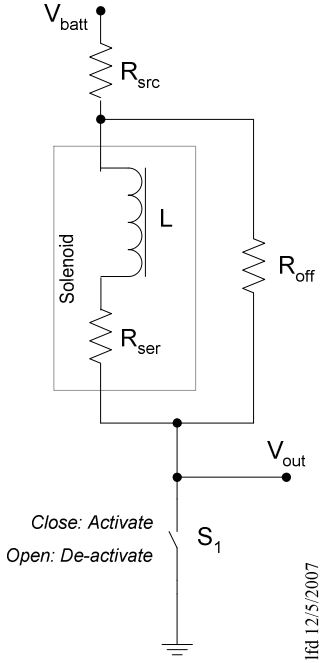

Figure 6: Simple Inductive Circuit Model

The solution to the differential equation, for time from 0 to just before t_{SW} (shown as t_{sw}^{-}) changes and with an initial condition of zero current, is:

Equation 3: $i(t)_{t=0\rightarrow t_{SW}^{-}} = \frac{V_{batt}}{(R_{src} + R_{ser})}\left(1 - e^{\frac{-t}{\tau_{act}}}\right)$

Where: $\tau_{act} = \frac{L}{(R_{src} + R_{ser})}$

After the inductor is energized, switch S_1 is moved to the open position (to de-energize the solenoid) and the differential equation becomes (from time t_{SW} to infinity with an initial current flowing):

Equation 4: $$L\frac{di}{dt}\bigg|_{i_0=i_{init}} = i\times(R_{ser}+R_{off})$$

The initial current flow (starting at time t_{SW}, given that $t_{SW} > 3x\tau_{act}$) is calculated using Ohm's law and sets the initial condition for the differential equation above as follows:

Equation 5: $$I_{init}\big|_{t_{sw}>3\tau_{act}} = \frac{V_{batt}}{(R_{src}+R_{ser})}$$

The solution to the differential equation is:

Equation 6: $$i(t)_{t_{SW}\to\infty} = I_{init}\times e^{-\left[\frac{t-t_{sw}}{\tau_{deact}}\right]}$$

Where: $$\tau_{deact} = \frac{L}{(R_{off}+R_{ser})}$$

As an example, the following component values will be used:

Component	Value	Units
R_{src}	10.0	mΩ
V_{batt}	14.0	Volt
L_{coil}	2.15	mH
R_{ser}	2.07	Ω
R_{off}	15.5	Ω

Figure 7: Components for an Inductive Load Example

The current flow and voltage response is shown in Figure 8 that follows (plot [A] covers the entire time range, while plot [B] focuses on the flyback time only).

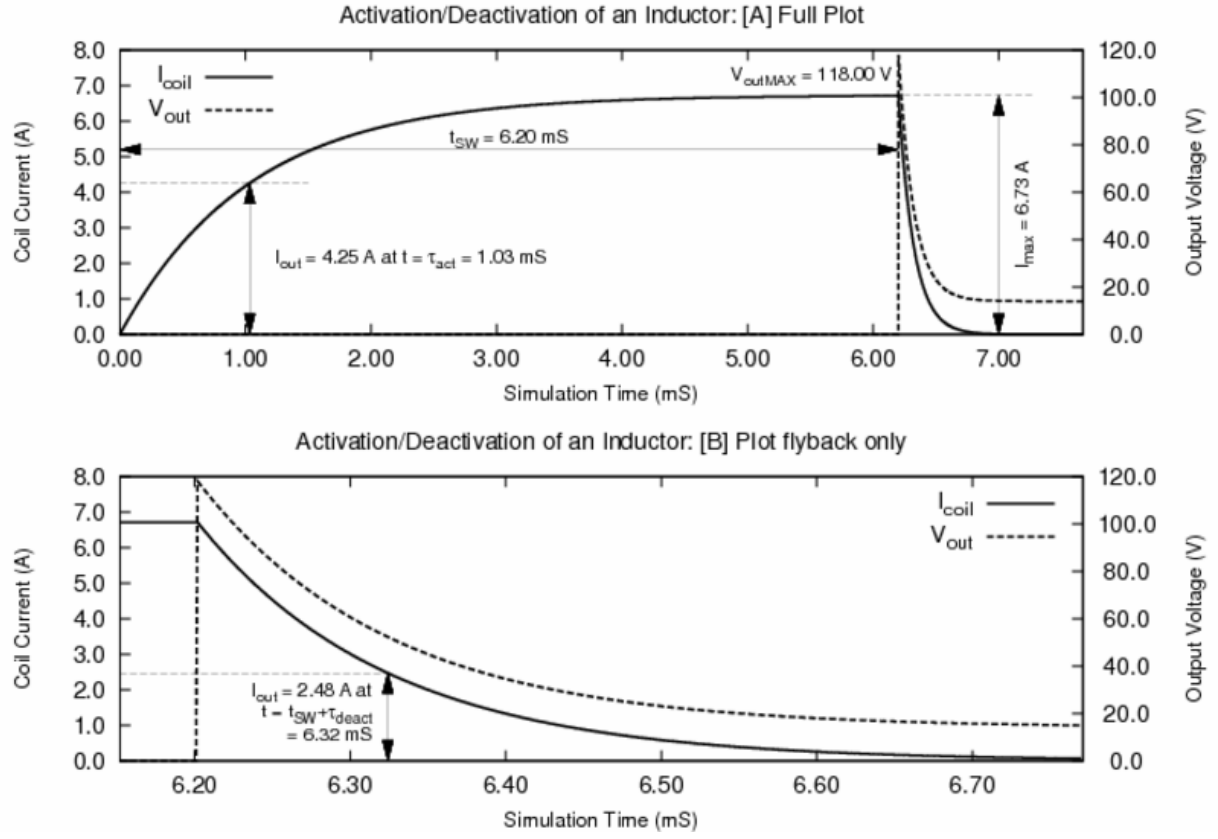

Figure 8: Simplified Inductor Circuit, Simulation Results

The plots in Figure 8 show that the inductor current rises exponentially from zero to the maximum ($I_{max} = V_{batt}/[R_{ser}+R_{src}]$) with a time constant of τ_{act}. Once the switch is moved to the de-energize position, the current starts to drop exponentially by a new time constant, namely τ_{deact}, and also, the V_{out} voltage immediately climbs to a high of over 115 volts (under these circumstances) and drops exponentially to V_{batt} at the same time constant.

The analysis just presented provides a qualitative understanding of how solenoids operate and the relative levels of voltages and currents to expect. However, the use of an analog circuit simulator (such as one of many variations of SPICE based CAE products) is a more practical method for evaluating solenoid operation while being driven by complex controllers such as the FDMS2380.

The complexity of real solenoids and of practical drivers (like the FDMS2380) makes it challenging (if not impossible) to derive closed form equations to predict operational results that would accurately match those obtained in a laboratory or in a real application. The preceding analysis does, none the less, give some insight into the operation of a solenoid in real world applications. There are, however, calculations that can be performed to simplify the design and implementation of solenoid applications which will insure that the solenoid and the FDMS2380 will operate within device limits (and provide an operational margin of error). These calculations will be reviewed in various sections of this applications note.

Force Produced by a Solenoid

As mentioned previously, the solenoid is a device that converts electrical energy[2] into mechanical energy. The derivation of the equation relating electromagnetic quantities to the resultant force can be found in the appendix - "*A.2: Derivation of Equations for Solenoid Force Calculations*" (starting on page 43). The final result (see Equation 34) is copied here:

$$f(x) = -\frac{1}{2}\Phi^2 \frac{d\Re}{dx}$$

where:

- $f(x)$ is force as a function of distance
- Φ is flux;
- $\Re$ is reluctance;
- x is distance

This general equation will be applied to specific mechanical configurations to determine the relationship between the force and other parameters of the solenoid.

The first solenoid configuration to be analyzed is the ***flapper*** style as shown in Figure 9. The diagram shows that the solenoid coil is wound on an *"E" like* shaped core made of steel laminated plates. The magnetic flux path (labeled "ϕ") has a circular cross sectional area (radius "a"). The rectangular moveable armature is on a pivot that allows the gap (labeled "g") to be changed based on the magnetic force. The derivation assumes the following simplifying assumptions:

- The coil is never driven into saturation[3]
- $g > 0$ (i.e., the gap never goes to zero)
- Reluctance of core is ignored[4]
- Core eddy currents[5] are ignored[6]

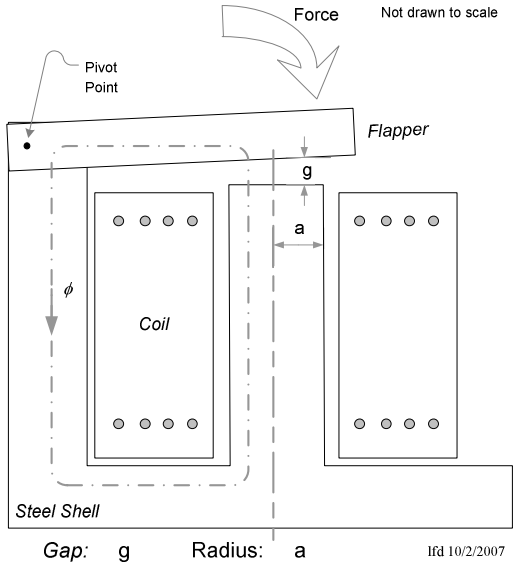

Figure 9: Flapper Style Solenoid - Mechanical Configuration

Beginning with Equation 34 and then substituting Rowland's law equivalent ($\Phi = \Im/\Re$) results in:

Equation 7: $$f(x) = -\frac{1}{2}\left(\frac{\Im}{\Re}\right)^2 \frac{d\Re}{dx}$$

[2] The terms energy and work can be used interchangeably.

[3] This is justified because additional current, beyond core saturation, would result in a diminishing increment in force and yet would require a disproportional amount of extra power.

[4] μ_r for silicon GO steel is 40,000 and so ignoring the reluctance of the core is justified

[5] Eddy currents, see "A.6: Definition of Terms and Symbols" for details

[6] Since the core is laminated, this assumption is justified

where:

f(x) is force as a function of distance

$\Im$ is magnetomotive force or mmf (with units Ampere-Turns);

$\Re$ is magnetic reluctance (with units Ampere-Turns/Weber);

x is distance (with units meters)

The reluctance of the flux path is just the reluctance of the gap since it is reasonable to ignore the reluctance of the core. Reluctance is defined as the length of the path divided by the area multiplied by the permeability of the area. In this case, the length of the path is "g", the permeability is that of air (μ_0) and the area is the area of a circle, which results in:

Equation 8:
$$\Re = \frac{\ell}{\mu \bullet A} = \frac{g}{\mu_0 \pi a^2}$$

Inspecting Equation 8 shows that as the gap gets larger, the reluctance increases linearly and also note that the applied force will act to try and reduce the reluctance. That is, the force will work towards making the gap smaller.

Reluctance (see Equation 8) and the derivative of reluctance are needed and the derivative of reluctance for this configuration is:

Equation 9:
$$\frac{d\Re}{dg} = \frac{d}{dg}\left(\frac{g}{\mu_0 \pi a^2}\right) = \frac{1}{\mu_0 \pi a^2}$$

Finally, Equation 8 and Equation 9 are substituted into Equation 7 resulting in:

Equation 10:
$$f(x) = -\frac{1}{2}\left(\frac{\Im}{\left(g/\mu_0 \pi a^2\right)}\right)^2 \frac{1}{\mu_0 \pi a^2} = -\frac{\pi \mu_0}{2}\left(\Im \frac{a}{g}\right)^2$$

Exploring Equation 10 reveals that the force is inversely proportional to the square of the gap distance. A plot of force and reluctance for a given set of solenoid parameters is shown in Figure 10.

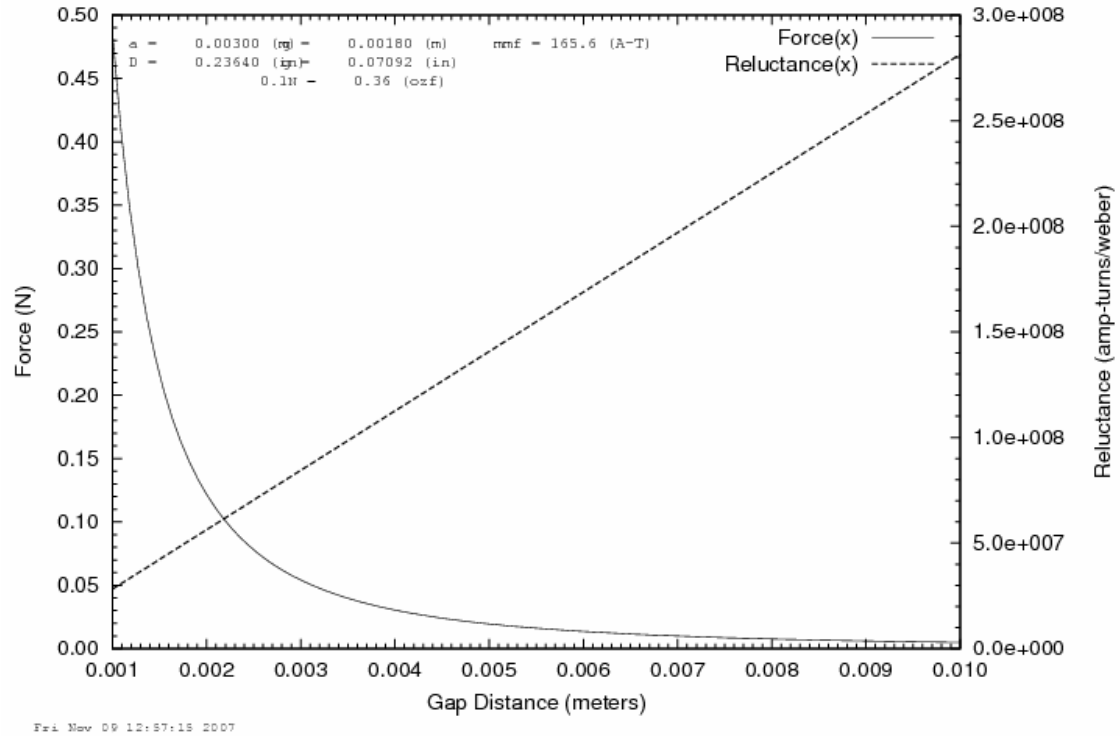

Figure 10: Magnetic Force and Reluctance Vs. Gap - Flapper Style Solenoid

The second mechanical configuration, the ***open ended plunger*** style, is displayed in Figure 11. The plunger is cylindrical with a radius "a" and is fully engaged when the stroke "v" is at a distance of "h" as measured from the inside bottom of the surrounding core (the disengaged position is when $v=0^+$). Furthermore, the plunger is centered in the core with a clearance of "c" evenly around the plunger.

As with the previous section, the starting point is Equation 34, Equation 7 and the general part of Equation 8. Also, as in the last example, all the assumptions hold here as well.

With this mechanical arrangement, the reluctance is the sum of two parts – the reluctance of the bottom of the plunger (a constant throughout the stroke) and the top of the plunger (the area changes with the stroke position).

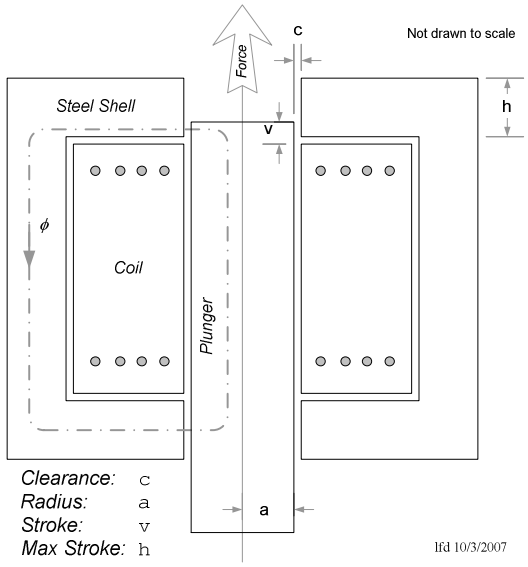

Figure 11: Open Ended Plunger Style Solenoid - Mechanical Configuration

The reluctance is expressed mathematically as:

$$\textbf{Equation 11: } \Re = \frac{\ell}{\mu \bullet A} = \frac{c}{\mu_0 2\pi a h} + \frac{c}{\mu_0 2\pi a v}$$

To clarify, the length in each case is simply the gap distance "c" and the area is the circumference multiplied by the height (the height is "h", a constant, in one case and "v", a variable, in the other). Notice that to make the reluctance smaller, the stroke distance "v" must get larger.

Next, the derivative of $\Re$ is needed:

$$\textbf{Equation 12: } \frac{d\Re}{dv} = \frac{d}{dv}\left(\frac{c}{\mu_0 2\pi a h} + \frac{c}{\mu_0 2\pi a v}\right)$$

Simplify and rearrange terms:

$$= \frac{c}{2\pi a \mu_0}\left(-\frac{1}{v^2}\right)$$

Finally, Equation 11 and Equation 12 are substituted into Equation 7 to get the force as a function of stroke distance "v", which, with some additional algebraic manipulations, results in the following equation:

Equation 13:

$$f(v) = -\frac{1}{2}\left(\frac{\Im}{\frac{c}{\mu_0 2\pi a h} + \frac{c}{\mu_0 2\pi a v}}\right)^2 \frac{c}{2\pi a \mu_0}\left(-\frac{1}{v^2}\right)$$

$$= \pi a \mu_0 \frac{\Im^2 h^2}{c}\left(\frac{1}{v+h}\right)^2$$

Some insight into the behavior of reluctance and force over the stroke for this mechanical configuration can be gleaned by studying the following plot for a particular set of solenoid parameters.

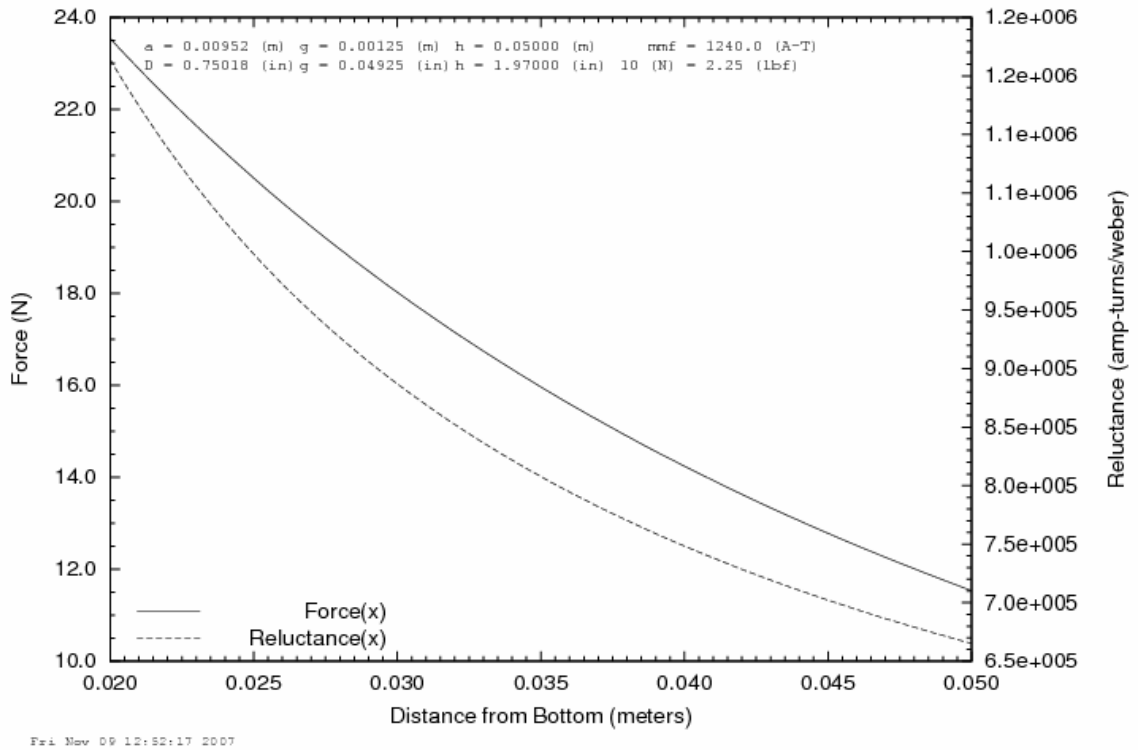

Figure 12 : Magnetic Force and Reluctance Vs. Stroke - Open Ended Plunger Style Solenoid

Notice that the maximum force (and reluctance) occurs when the value of "`v`" is the smallest and as the distance increases, the force diminishes. This is totally different from the previous case.

In general, therefore, the force equations have to be derived for each different mechanical configuration to determine how the force and reluctance will react to motion of the solenoid from the engaged to the disengaged positions.

Practical Considerations

As discussed in the previous section, heat dissipation within the solenoid must be taken into consideration to avoid solenoid damage as well as the resulting changes in coil resistance.

For example[7], a solenoid coil with a 1⅞ inch outer diameter, a ¾ inch inner diameter and a length of 1½ inches wound with about `450` turns of `#20` magnet wire would have a resistance of approximately `1.6`Ω at `20°C`. Over the entire automotive temperature range, the resistance would change from about `1.2`Ω to `2.4`Ω (about a `2:1` change overall).

Consult the solenoid manufacturer for the parameters specific to the solenoid being used and the specific application details.

The FDMS2380 was designed to control a solenoid using pulse width modulation (PWM) techniques. PWM techniques are used to control the coil current and thus the applied force, which in turn controls the power consumed by the solenoid as needed by the application (a great deal more on this issue is available in following sections).Generally, the `InB` pin is used for the PWM signal. By controlling the duty cycle of the applied voltage, the coil current and thus the solenoid force can be manipulated (more details about this are found later in this application note). The highest PWM frequency can be calculated using data sheet values for $t_{d(on)}$, t_r, $t_{d(off)}$ and t_f (consult the *Switching Characteristics* section of the latest data sheet for the most up-to-date values). The lowest PWM frequency is determined (mostly) by analyzing the thermal time constant of the solenoid coil and the FDMS2380 package.

Determining the minimum PWM period[8], (and also the minimum duty cycle) of the FDMS2380 can begin by considering the waveform shown in Figure 13.

[7] See Appendix "*A.1: Example Estimating Coil Wire Length and D. C. Resistance Change over* Temperature" for details.

[8] Notice, from Figure 13, that the minimum command pulse width (InB_{min}) applied to `InB` should be at least: $InB_{min} \geq t_{d(on)}+t_r$ (the actual full ON time at the output, in this case, will be $t_{d(off)}$).

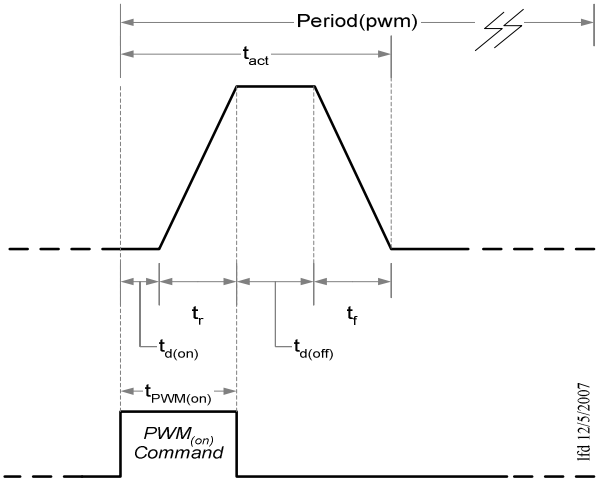

Figure 13: Parameters of Interest - Maximum PWM Frequency (which means minimum period)

From Figure 13 the parameter $t_{d(on)}$ is the output turn-on delay, the parameter t_r is the rise time of the output, $t_{d(off)}$ is the parameter for output turn-off delay and t_f is the output signals fall time (the specific test conditions are stated in the latest FDMS2380 data sheet). Realize that neither $t_{d(on)}$ nor $t_{d(off)}$ are pure delay elements. That is, in order to get full voltage at the FDMS2380 output pin, the command to the FDMS2380 must last for at least the sum of $t_{d(on)}$ and t_r ($t_{d(off)}$ and t_f are similar for turning the device off). The FDMS2380 was designed specifically with this timing feature which the internal logic uses to control the rise/fall times of the output signals and thus supporting the mitigation of EMI related issues.

One method, to proceed with determining PWM drive limits is to perform the set of calculations that follows.

1. Choose the number of different intermediate coil current commands needed, N_{iv} (i.e., each different duty cycle will command a different average coil current and thus magnetic force). For example, if $N_{iv}=2$ is chosen, there would be four (4) levels available: full off, two (2) intermediate values and full on. That is, the total number of commands is calculated as $N_{iv}+2$.
2. Choose a value for Δt where $\Delta t \geq t_{d(off)}$ and calculate the PWM period (λ_{pwm}):
   $\lambda_{pwm} = t_{d(on)}+t_r+(N_{iv}+1)\Delta t+ t_f$
   $f_{pwm} = 1/\lambda_{pwm}$
   The maximum value of Δt is determined by parameters including the thermal time constant of the solenoid, the thermal time constant of the FDMS2380 as mounted and others.
3. Calculate each of the command lengths as (i.e., duty cycle values):
   $t_{PWMact[0]} = 0$ (Full OFF)
   $t_{PWMact[j]} = t_{d(on)}+t_r+j\Delta t$
   (where: $1 < j \leq N_{iv}$ and ON Duty Cycle = $t_{PWMact[j]}/\lambda_{pwm}$)
   $t_{PWMact[Niv+1]} = \lambda_{pwm}$ (Full ON)
4. Calculate the average current[9] for each of the commands in the previous step as:
   $i_0 = 0$ (Full OFF)
   $i_j = (V_{batt}/R_{coil})*(t_{PWMact[j]}/\lambda_{pwm})$ $(1 < j \leq N_{iv})$
   $i_{Niv+1} = V_{batt}/R_{coil}$ (Full ON)
5. Verify that the calculations hold for both typical and worst case parameters.

For example, using the following FDMS2380 timing parameters:

$t_{d(on)} = 7.0\mu S$, $t_r = 6.5\mu S$,
$t_{d(off)} = 8.3\mu S$ and $t_f = 3.0\mu S$

and the following operating parameters:

$N_{iv} = 2$,
$\Delta t = 42.0\mu S$ and
$V_{batt} = 14.0$ V
$R_{coil} = 1.2\Omega$ (therefore $I_{max}=11.67A$)

First calculate the PWM parameters:

$\lambda_{pwm} = 142.5\mu S$
$f_{pwm} = 7.0kHz$

Now calculate the command lengths and the resultant average coil currents:

$t_{act[0]} = 0$ $i_0 = 0$ (Full OFF)
$t_{act[1]} = 55.5\mu S$ $i_1 = 4.54A$ (38.9%)
$t_{act[2]} = 97.5\mu S$ $i_2 = 7.98A$ (68.4%)
$t_{act[3]} = 142.5\mu S$ $i_3 = 11.67A$ (Full ON)

As well as the calculations above, the average coil currents should be calculated for minimum and maximum V_{batt} to insure there is sufficient force under all conditions. These results are shown schematically in Figure 14.

[9] As will be shown later, the ON duty cycle multiplied times the maximum current equals the average current applied to the coil.

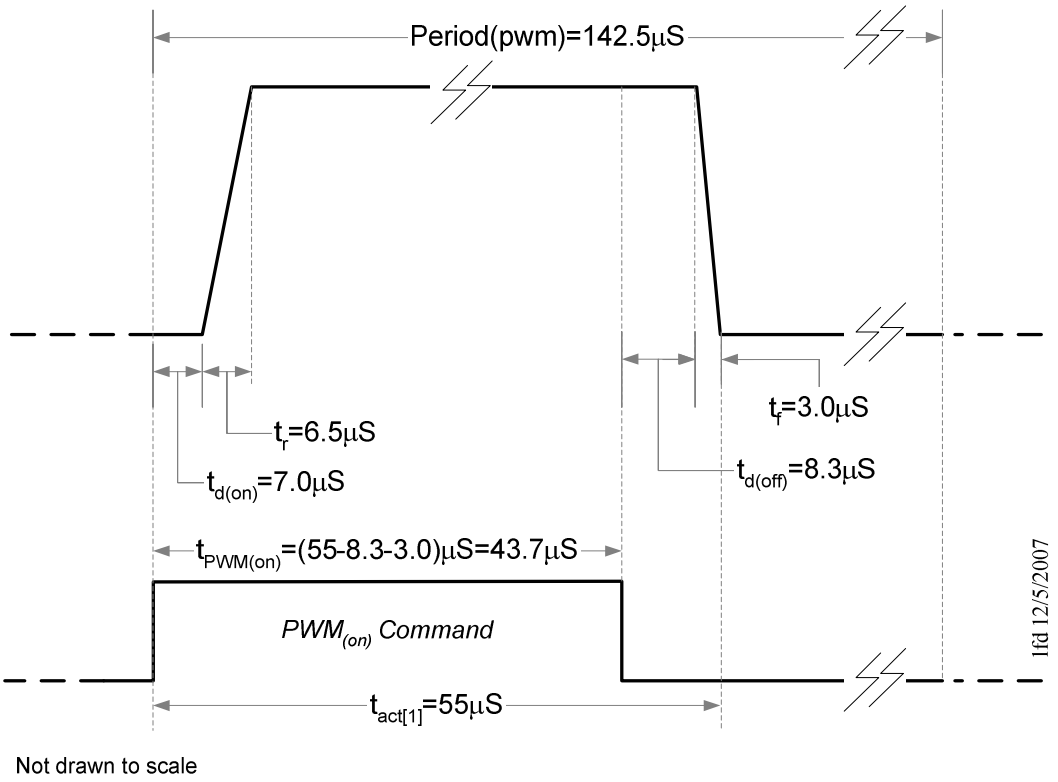

Figure 14: Example PWM Parameters ($t_{act[1]}$)

The use of the delay and transition times is not generally critical as they typically will not change the results. In this example:

7.0μS+6.5μS+8.3μS+3.0μS = 24.8μS

This total is <20% of the PWM period (in this example, 24.8μS of 142.5μS).

It should be noted that this is not the only method to determine the PWM parameters, but other methods must take into account the FDMS2380 timing parameters, its associated manufacturing tolerances and other applications parameters.

Another practical consideration that is beneficial to mention is the notion of using two or more FDMS2380 channels in parallel (i.e., attaching the output pins of each different channel or device to the others). Paralleling two or more FDMS2380 channels to improve current handling capabilities should not be done because the device's fast turn-off mode parameters could not be matched from channel to channel (or device to device) over the complete temperature range. That is, it is not recommended to tie any two OUT pins together in an effort to gain higher capability than is available in a single channel.

FDMS2380 Description

As stated earlier, the FDMS2380 is a dual low side high-power driver designed to operate with inductive loads and has on-chip logic to simplify the implementation. The on-chip logic has features to detect several common faults, in addition to flexibly managing the inductive loads in several modes. The device is packaged in an 18-pin power QFN (PQFN[10]) package with a symmetrical pin-out that allows the device to be installed in either orientation. In summary:

- Protection Features
  - Over Current Protection
  - V_{batt} Over and Under Voltage Protection
  - Over Temperature Protection
- Diagnostic Features
  - Per Channel Diagnostic Signal
  - Open Load Diagnostic
  - Soft Short (Ground Fault) Diagnostic
  - Flyback Duration Reporting
- Electrical Characteristics
  - 6V to 26V Operation
  - 30mΩ Typical $R_{ds(on)}$ Excitation

[10] See appendix "*A.6: Definition of Terms and Symbols*" under the term PQFN for more information about packaging

- 60V Typical Load Clamp[11]
- CMOS Compatible Input Levels

- Thermal Characteristics
  - PQFN Package
  - 7W Total Package Dissipation

More details can be found in the device data sheet (see reference #1).

Signal Descriptions

Shown in Figure 1 are the external connections to the device as well as the pin numbers (numbers shown in parentheses) for each signal. There are connections to power (V_{batt} and Gnd) and the load for each channel (Out_1 and Out_2). Notice that the ground connections are electrically independent for each channel and are normally tied together with traces. There are two logic inputs for each of the two channels for selecting operational modes (InA_1, InB_1, InA_2 and InB_2) and an open drain diagnostic signal for each channel ($Diag_1$ and $Diag_2$) used to identify faults. The diagnostic signal can also be used to measure parameters about the operation of the solenoid (e.g., flyback duration, etc.). Since the diagnostic signal is open drain, a 10kΩ pull-up resistor is required (pulled up to the +5V logic supply[12]).

A top view of the FDMS2380's physical pin-out, which shows the signal names, is illustrated in Figure 15.

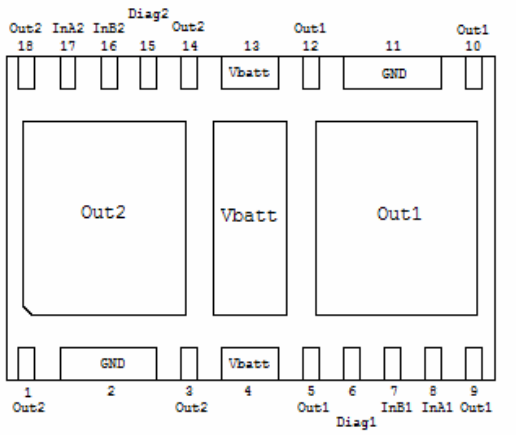

Figure 15: FDMS2380 Physical Pin-out with Signal Names (Top View, Not to Scale; See data sheet for land pattern details)

The logical blocks within the FDMS2380 are shown in Figure 16. The detail shown in the diagram for channel 1 is identical to that of channel 2. Notice that there are four (4) PowerFET's, one for excitation, one for recirculation for each of two channels and all are internal to the package making the device a completely integrated solution for managing inductive loads such as solenoids.

The five (5) sensing blocks (*Vreg Block, Soft Short, Open Load, Over Temperature* and *Over current*) are designed to sense a specific fault condition (e.g., Over Temperature, etc.) and continually report results to the *Control Block* for action.

The *Diagnostic Control* block receives fault condition indications, filtered by the *Control Block*, and drives the channel's diagnostic pin. The role of this block is to generate the appropriate diagnostic pulse timings as well as to generate the blanking pulse[13] for insuring a pulse is generated in special cases (see Figure 19 for details).

The *PMOS Driver Block* and *NMOS Driver Block* produce signals specifically intended to drive the PowerFET gates as directed by the *Control Block*. Additionally, these blocks control the rise and fall times of the gate signals so as to help reduce EMI related problems at the outputs.

The block labeled "*Control Block*" is the element that manages the entire channel. It interprets the commands from the InA and InB pins, monitors fault conditions (e.g., over temperature, over current, etc.), at the appropriate times it generates signals for the DIAG pin and commands both PowerFET's. A state diagram shown in Figure 18 describes the simplified operation of this block (error free circumstances only), while Figure 19 shows the more complete state diagram including all fault conditions. Associated with the state diagram is the table in Figure 17 that explains how the PowerFET's are activated for each of the major operational modes.

The next section describes the FDMS2380 modes of operation.

[11] The voltage shown is a minimum value for $V_{out(cl1)}$ (consult Data Sheet for more details) and is for load dump protection.

[12] It is very important not to pull up the Diag pin beyond $V_{diag(max)}$ (a value to use is 8V, but it is best to check the data sheet)

[13] A *blanking pulse* is used to insure that a second fault is indicated when a previous one is already being indicated. See "A.6: Definition of Terms and Symbols" for more details.

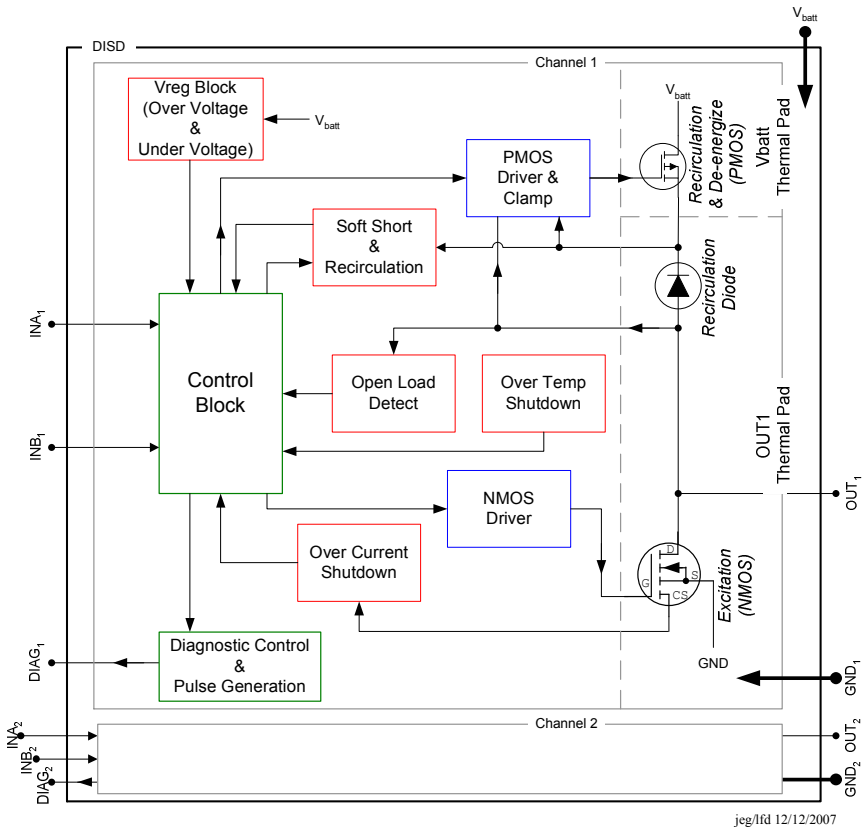

Figure 16: FDMS2380 Internal Logical Block Diagram

Modes of operation

Given the application diagram shown in Figure 42 on page 40, the operation of the FDMS2380 can be described through its operating modes and by further dividing the modes into two categories – *Normal Operations* and *Fault-Condition* modes.

Normal Operation

Focusing on just normal operations, those FDMS2380 modes are listed in the Figure 17 table. This table shows how the two PowerFET's are driven in each of the modes.

The term "*ON*" means that the gate of the PowerFET is driven so that the drain to source impedance is at its lowest (i.e., $R_{ds(on)}$) value whereas "*OFF*" means the highest impedance. "*Clamped*" is a term[14] that means the device is configured to regulate the voltage between drain and source to a high constant voltage (i.e., $V_{out(cl2)}$). When the NMOS device is turned on, regardless of whether the PMOS is on or off (the recirculation diode isolates the path), current flows through the load, thus energizing the magnetic field.

Mode	*Excitation Path (NMOS)*	*Recirculation Path (PMOS)*
Standby (InA=0; InB=0)	off	off
Excitation (InA=1; InB=1)	**ON**	ON
Recirculation (InA=1; InB=0)	off	**ON**
Fast Discharge (InA=1➔0; InB=0)	off	Output clamped to $V_{out(cl2)}$

Figure 17: NMOS/PMOS Control by Operational Mode[15]

A state diagram of how the FDMS2380 transitions from mode to mode, under no-fault conditions, is shown in Figure 18. The combination of the two diagrams (table shown in Figure 17 and state diagram in Figure 18),

[14] There are two clamp voltage levels for each of the two FDMS2380 channels. $V_{out(cl2)}$ discussed here and $V_{out(cl1)}$ mentioned elsewhere. That is, the "1" and "2" subscripts do not refer to channels, but different functionality. See "*A.6: Definition of Terms and Symbols*" for more details.

[15] Refer to the data sheet (reference #1) for a more comprehensive table which includes fault conditions.

describes how the FDMS2380 operates and how it affects the attached load.

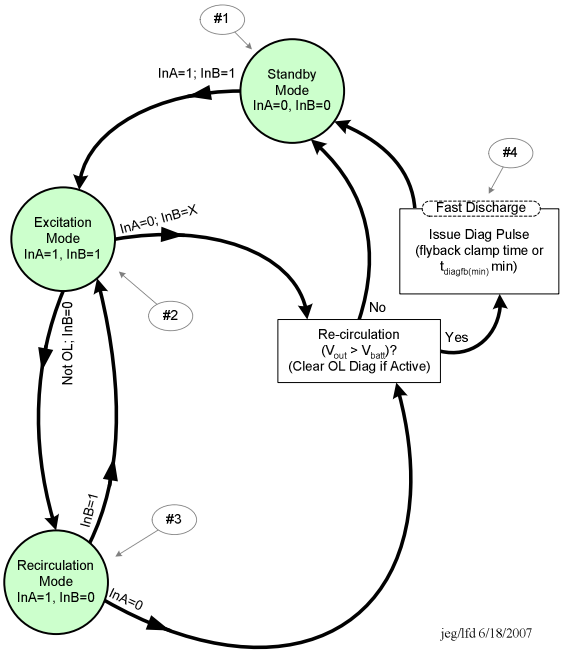

Figure 18: FDMS2380 State Diagram (Normal Operations - No Fault-Conditions)

The following discussion refers to the state diagram as shown in Figure 18. The *Standby Mode* (labeled as #1) is entered at initial start-up and any time when the solenoid is to be disengaged (e.g., moved to its rest position). The *Standby Mode* is commanded by setting both InA and InB to logic zero ($signal \leq V_{il}$). In this mode, as shown in Figure 17, both PowerFET's are put in the high impedance or OFF state. Going to the *Excitation Mode* (engaging the solenoid; the state labeled as #2) is accomplished by setting both InA and InB to logic one ($signal \geq V_{ih}$). The NMOS device is then turned fully on, while the PMOS device is also turned fully ON (notice that the recirculation diode prevents current from flowing to ground through the conducting PMOS device). In typical applications, engaging the solenoid involves two phases – full current for pulling in the solenoid quickly and a lower current value for holding the solenoid in place (the engaged position). The lower current value is achieved using PWM technique by toggling the InB pin between logic one and zero while InA remains high. When in the *Excitation Mode* (both InA and InB are at logic one), the FDMS2380 is moved to the *Recirculation Mode* (labeled as #3) by setting InB to logic zero (in this mode, the NMOS device is turned fully OFF while the PMOS device remains fully ON). As dictated by the application's current needed, at some time, InB is once more changed to logic one and the FDMS2380 transitions to the *Excitation Mode* again. Finally, when the solenoid needs to be disengaged, both InA and InB are set to logic zero and the device transitions to the *Fast Discharge Mode* (labeled as #4) and then to the *Standby Mode* or directly to the *Standby Mode* under the conditions as shown in Figure 18.

The fast discharge mode (labeled #4 and only entered if the output voltage is greater than[16] V_{FB}) issues a Diag pulse whose duration is equal to a minimum of $t_{diagfb(min)}$ or a pulse width equal to the time for the output voltage to drop to V_{batt}. This feature can therefore be used to determine in situ load parameters for system diagnostic capability. So, for example, shorted turns within the solenoid could be detected under the proper conditions. That is, shorted turns would mean a lower coil resistance which would cause a higher maximum coil current. This higher maximum coil current would take a longer time to discharge which would result in a longer diagnostic pulse width. Then again, fewer turns, due to a shorted turns fault condition, would mean a reduction in inductance (depending on the physical construction, inductance could be proportional to the square of the number of turns) and since the time constant is directly proportional to the coils inductance, the discharge rate would increase. This faster discharge rate would be reflected in a shorter diagnostic pulse during flyback. The exact timing would depend on the details of the coil construction and the details of the fault condition.

As just discussed, notice that changes in the electrical parameters of the coil as a result of faults produce changes in opposite directions (i.e., $\tau = L/R$, both L and R can be effected by a fault condition). Consequently, the use of flyback timing as a diagnostic capability has to be evaluated using the unique parameters for each particular application.

One major advantage of using the FDMS2380 is that it can detect fault conditions, protect itself and report detected faults through a signal pin. The fault conditions and related data sheet parameters are:

- V_{batt} over voltage ($V_{batt(ov)}$)
- V_{batt} under voltage ($V_{batt(uv)}$)
- Junction over temperature ($T_{j(tsd)}$)
- Output over current ($I_{OUT(trip)}$)
- Output ground fault ($V_{out(ss)}$)
- Output open load (I_{ol})

Figure 18 shows a state diagram for normal operation while Figure 19 shows the complete state diagram for all possible conditions including handling of fault conditions. Following is more discussion on the operation of the FDMS2380 under fault conditions. However, the FDMS2380 data sheet should be consulted for a complete description of how the FDMS2380 responds to the fault conditions and for the related device parameters.

[16] $V_{out}-V_{batt}>V_{FB}$; Check data sheet for value, but V_{FB} is typically 23V.

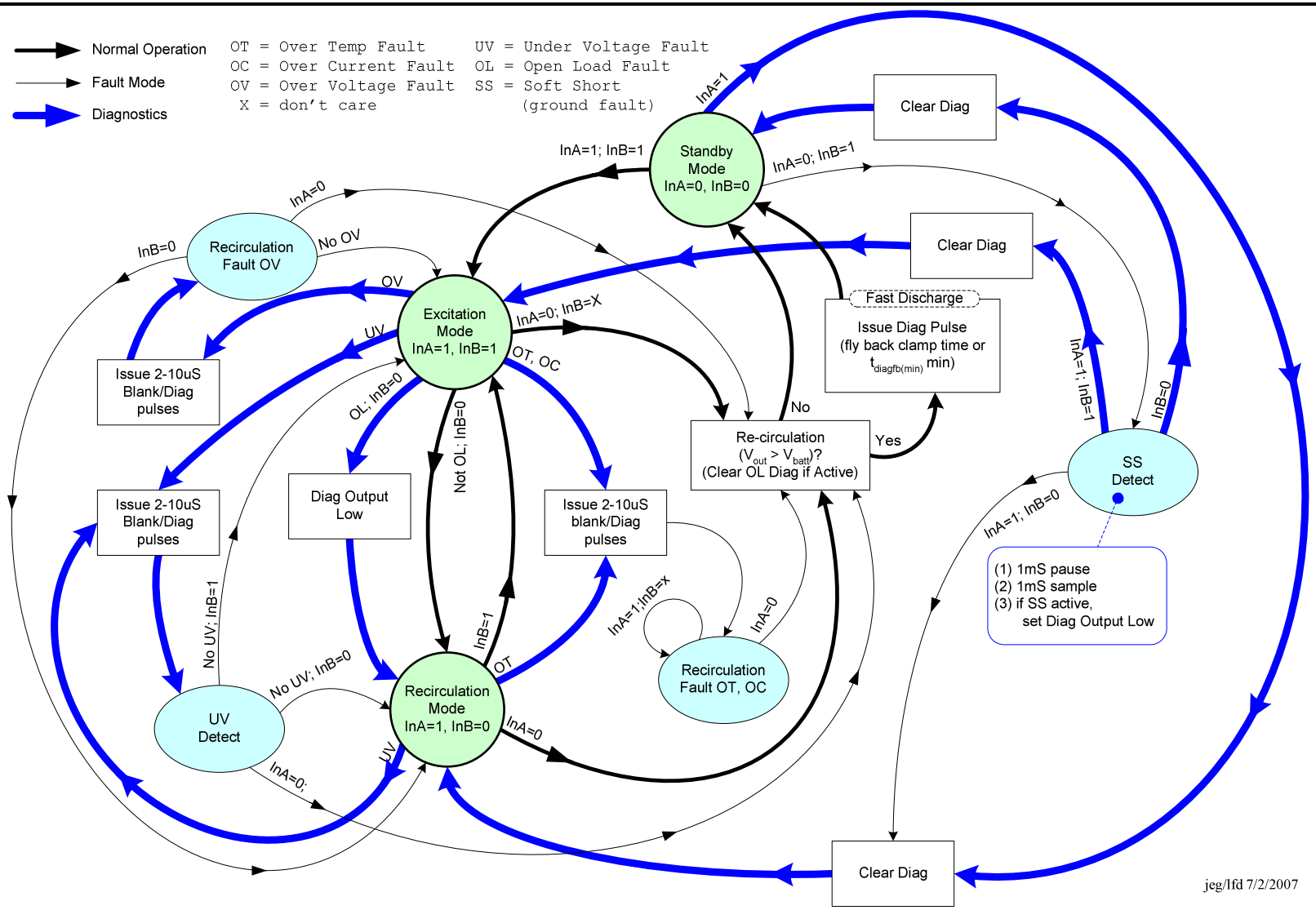

Figure 19: FDMS2380 State Diagram (all modes of operation)

Soft Short Operation

The soft short capability is a special mode used to detect conditions, on either or both channels, where a ground fault exists between the output pin and ground (see Figure 20).

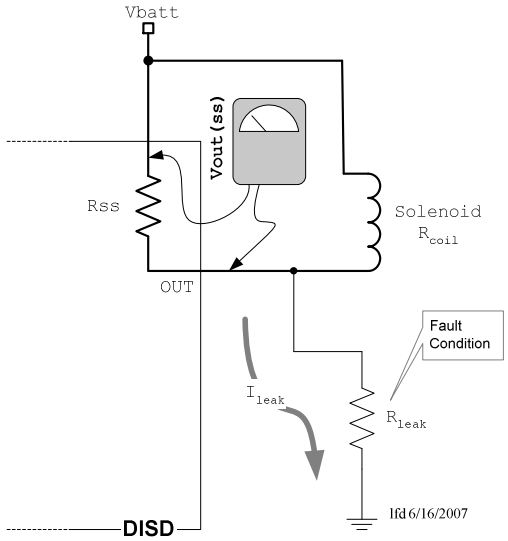

Figure 20: Soft Short Fault Condition

If a ground fault exists in an application through some failure mode, it could be severe enough to cause the solenoid to turn on and thus be uncontrollable by the FDMS2380, so it is important to detect the condition and take appropriate action. The value of leakage current (I_{leak}) to trip the diagnostic signal can be calculated as follows.

Equation 14: $$I_{leak} \geq \frac{V_{out(ss)}}{R_{ss}}$$

For example, given nominal parameter values of R_{ss} = 70Ω and $V_{out(ss)}$ = 0.43V, then $I_{leak} \geq 6.1mA$. Leakage currents sufficiently high to trip the soft short signal can vary from 3.3mA to 12.0mA depending on the specific device parameters (i.e., manufacturing variations, variations in operating temperature, etc.).

The soft short mode for a particular channel, as shown in Figure 19, is entered from the standby mode by setting InA low and InB high and then monitoring the Diag pin for a high to low transition. If there is a soft short condition, the Diag pin will transition within 1.5mS to 4.0mS. The soft short mode test current is applied for only ~2mS, so there is little to be concerned about with respect to power dissipation in the fault load. Exiting this mode (see Figure 21 for details) is accomplished by changing the state of InA or InB (e.g., go to Standby mode, Excitation mode or Recirculation mode).

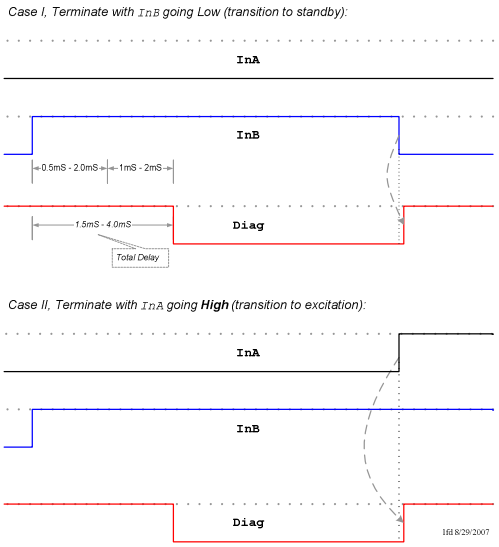

Figure 21: Exiting from Soft Short Mode

It is important to fully de-energize the load before entering soft short mode. Also, a delay of at least 10mS is needed between the activation of multiple sequential soft short modes.

Open Load Operation

The *Open Load Fault* condition is sampled with a transition from the *Excitation Mode* (i.e., InA=InB=1) to the *Recirculation Mode* (i.e., InA=1; InB=0) and the conditions must be present on the falling edge of InB. When present, the Diagnostic signal is brought low as long as InA is high except where there are other faults (i.e., OT, OC, OV, or UV). The Data Sheet parameter I_{ol} (300mA<Iol<800mA) specifies the minimum current that must be drawn to avoid the Open Load fault. So, for example, with V_{batt}=14V, a resistance of less than 17.5Ω (14V/0.8A) must be present between the output pins and V_{batt} to prevent open load fault conditions from being exhibited or with V_{batt}=6V, a resistance of less than 7.5Ω must be present.

Notice, however, that the previous analysis assumes a resistive load. For an inductive load, the current will rise exponentially according to the time constant L_{coil}/R_{coil}. So use the following parameters (under two different junction temperatures) as an example:

V_{batt} (V)	L_{coil} (mH)	$I_{out(OL)}$ (mA)[17]	Coil Temperature (°C)	R_{coil} (Ω)
Condition I				
14	3.03	450	20	1.62
Condition II				
8	3.03	430	150	2.45

The timing for a PWM frequency of 4kHz (i.e., period 250µS), with a 40% duty cycle is a 100µS ON and a 150µS OFF duration. Now calculate operational parameters:

τ (µS)	$I_{coil(max)}$ (A)	Charge Time[18] to $I_{out(OL)}$ (mS)	10% of $I_{coil(max)}$ (A)
Condition I			
1,870	8.64	0.100	0.864
Condition II			
1,240	3.27	0.174	0.327

Reviewing the table of operating conditions (shown above) reveals that under both conditions, a pull-in phase of one or more time constants in length will be enough time for the inductor to charge up well beyond the $I_{out(OL)}$ threshold value. In fact, also shown in the table, is that the pull-in phase can be just greater than 174µS, for no open load diagnostic pulse to be issued (which is a correct indication). However, when the *condition II* parameters are in effect and the device is in the steady state part of the hold phase with an ~10% duty cycle, the coil current is less than the $I_{out(OL)}$ threshold value (i.e., 327mA is less than 430mA) which appears to the FDMS2380 as an open load condition. In this case, the diagnostic pulse will be activated showing an open load condition. Notice that the FDMS2380 is operating as it should, but the application conditions are causing the false indication. Notice also that the $I_{out(OL)}$ threshold is an instantaneous determination and so the instantaneous I_{out} will dip below the average current value. This means that, the average current has to be increased somewhat beyond the $I_{out(OL)}$ value to eliminate an open load indication.

Worst case calculations need to be performed over the entire temperature range and over all other variable parameters that the system will operate under (e.g., minimum V_{batt}, maximum V_{batt}, etc.) to verify that false indications do not occur.

[17] Variation estimated from figure 17 in the data sheet

[18] The equation for the charge time is derived from Equation 3 by solving for "t".

Operation Under Other Fault Conditions

The four fault conditions of *V_{batt} Under Voltage, V_{batt} Over Voltage, Junction Over Temperature,* and *Over Current* are only reported when in excitation mode (i.e., InA=InB=1) and when active, issue a single 2-10µS Diag pulse. A blanking pulse[19] is issued by each reporting condition as needed (i.e., the Diag signal goes high for 2-10µS then low for 2-10µS).

Condition	Input		Response (Device Gate Drive)	
	InA	InB[20]	NMOS	PMOS
OT: Thermal Shutdown ($T_J > T_{J(tds)}$)	H	X	OFF	ON
OC: Current Trip ($I_{OUT} > I_{OUT(trip)}$)	H	H	OFF	ON
OV: Over Voltage ($V_{BATT} > V_{BATT(ov)}$)	H	H	OFF	ON
UV: Under Voltage ($V_{BATT} < V_{BATT(uv)}$)	H	X	OFF	OFF

Figure 22: OT, OC, OV, UV Fault Conditions

Presented in Figure 22 are four fault conditions with the associated data sheet parameters related to each, the driving conditions of each of the power devices and the respective input signal values that are needed for the power devices to be driven as shown in the figure's two far right side columns.

Refer to the latest FDMS2380 data sheet for further details of the operation of the *Under Voltage, Over Voltage, Over Temperature,* and *Over Current* fault conditions. Furthermore, the latest data sheet should be

[19] A *blanking pulse* is used to insure that a second fault is indicated when a previous one is already being indicated. See "A.6: Definition of Terms and Symbols" for more details.

[20] It is pointed out here that the fault is only reported on the diagnostic pin if InA and InB are high simultaneously

consulted to determine the most up-to-date values for the related parameters (e.g., $V_{batt(ov)}$, $T_{j(tsd)}$, etc.).

Flyback Operation

Another feature of the FDMS2380 that fits into the category of diagnostics is the flyback timing feature. The device synchronizes the width of the Diag signal, within limits, to the time it takes for the flyback voltage at V_{out} to fall from $V_{out(cl2)}$ to V_{batt} every time the device enters into the fast discharge mode. This can be used to analyze the condition of the attached inductive load (e.g., see Equation 47). At the extreme, for example, if the load becomes totally resistive and there is no flyback voltage, there will be no fast discharge flyback signal on the diagnostic pin. The timing and related voltages are depicted in Figure 23.

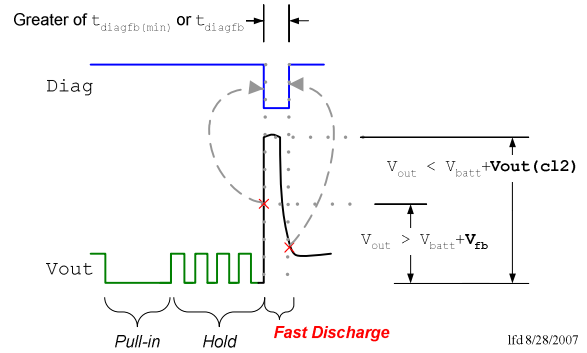

Figure 23: Flyback Timing

The figure shows that the width of the flyback diagnostic pulse is a minimum of $t_{diagfb(min)}$ (from the data sheet: $26\mu S<t_{diagfb(min)}<50\mu S$) and that the flyback voltage must be at least V_{fb} (from the data sheet: $22V<V_{fb}<33V$) above battery. A minimum flyback pulse width was designed into the FDMS2380 logic to give external controllers the ability to distinguish a flyback event from a signaled fault condition.

Thermal Considerations

Power is either supplied or absorbed as a FDMS2380 channel engages and disengages its attached inductive load (typically a solenoid). When engaging the load (FDMS2380 *excitation mode*), energy is supplied to increase the intensity of the magnetic field of the load as well as to supply power consumed by I^2R losses in the passive elements of the circuit. Perhaps less obvious is the fact that during load deactivation, energy is dissipated in the FDMS2380 device. That is, energy stored in the magnetic field of the load must be dissipated and it is dissipated by the FDMS2380 in the *fast turn-off mode*. Furthermore, when the FDMS2380 is in *recirculation mode*, losses in the collapsing magnetic field are absorbed by the FDMS2380. Sourcing or sinking of power through the FDMS2380 means that heat is generated within the device resulting in increasing die temperatures. The following section identifies what part of the chip generates heat under each major operating mode and outlines methods to estimate the magnitude of power dissipated.

The three (3) pads as shown in Figure 2 are the major thermal paths available for conduction of heat away from the die and out of the package. The excitation NMOS device and the recirculation diode (see the right side of Figure 16) are both thermally connected to the larger pad, while the PMOS device (recirculation and de-energizing circuit) is thermally connected to the smaller center pad. Given this layout, the following summarizes major heat generation for each of the three major FDMS2380 operating modes:

- Excitation mode (one pad per channel) — Large pad
- Recirculation mode (one pad per channel) and — Large pad, Small pad (single pad for both channels)
- Fast turn-off mode (single pad for both channels) and — Small pad, Large pad

This is shown diagrammatically in Figure 24.

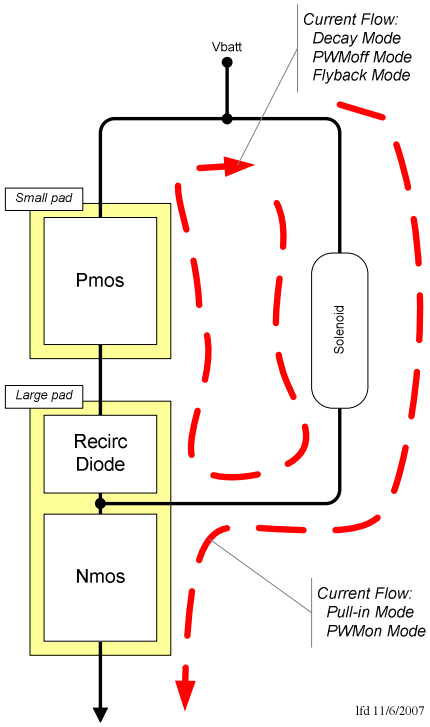

Figure 24: Current Flow and Heat Generating Components in each Operational Mode

A solenoid can be electrically engaged in several distinct phases and the process involves several related events as shown in Figure 25. First, there is an action command, by some high level controller, to engage or disengage the solenoid.

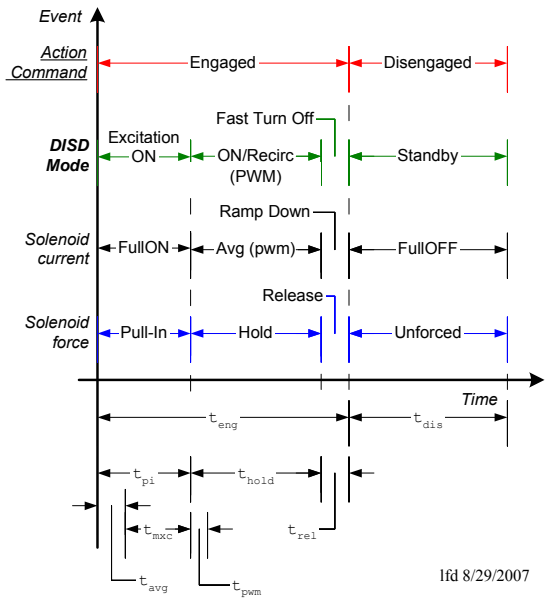

Figure 25: Phases of Engaging/Disengaging a Solenoid

In this example, the FDMS2380 is the controlling element in the circuit and to engage the solenoid, the FDMS2380 is normally commanded in three phases[21] – *Excitation ON*, *Excitation ON/Recirculation (PWM)* and *Fast Turn-Off*. When the solenoid is commanded to engage, the coil current (controlled by the FDMS2380) goes through three phases – *current ramp-up (Full ON)*, at least one *reduced current* setting using PWM techniques and finally *decaying* current (using the fast turn off mode of the FDMS2380). During the solenoids disengaged phase, no current flows through the coil (Full OFF). When engaged, the force applied by the solenoid goes through a related set of phases – *Pull-in* force, *Holding* force, and *Release* (or no force).

An advanced scheme for driving the FDMS2380 summarized in Figure 26.

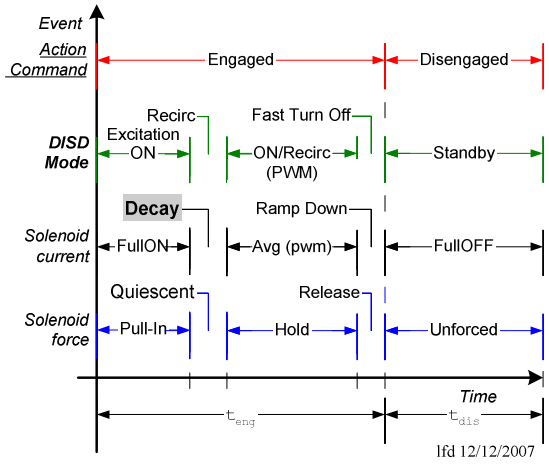

Figure 26: Driving a Solenoid – Advanced Command Phases

Comparing Figure 25 with Figure 26 it can be seen that the Advanced Command scheme adds a "*Quiescent*" phase after the "*Pull-In*" phase and before the "*Holding*" phase. During the Quiescent phase, the FDMS2380 is commanded into recirculation mode (i.e., `InA=1`, `InB=0`) and this quickly brings the coil current down to the level of the holding phase (more details on this issue can be found in the following paragraphs). The difference in the two driving schemes is speed. Using the Quiescent phase, instead of transitioning directly to the Holding phase, brings the coil current to the level during the Holding phase much faster.

The plot in Figure 27 is a simulation that implements the ordinary three phase command scheme (i.e., [1] Pull-in, [2] Hold, [3] Fast Turn-off and without a Quiescent phase). The plot shows that the time from the end of the Pull-in phase to the time when the coil current reaches the average value is `~4.2mS` (for this particular example, but the results vary with different system parameters).

[21] This is application dependent and so for some applications, the FDMS2380 might simply be turned full on and full off to control the load.

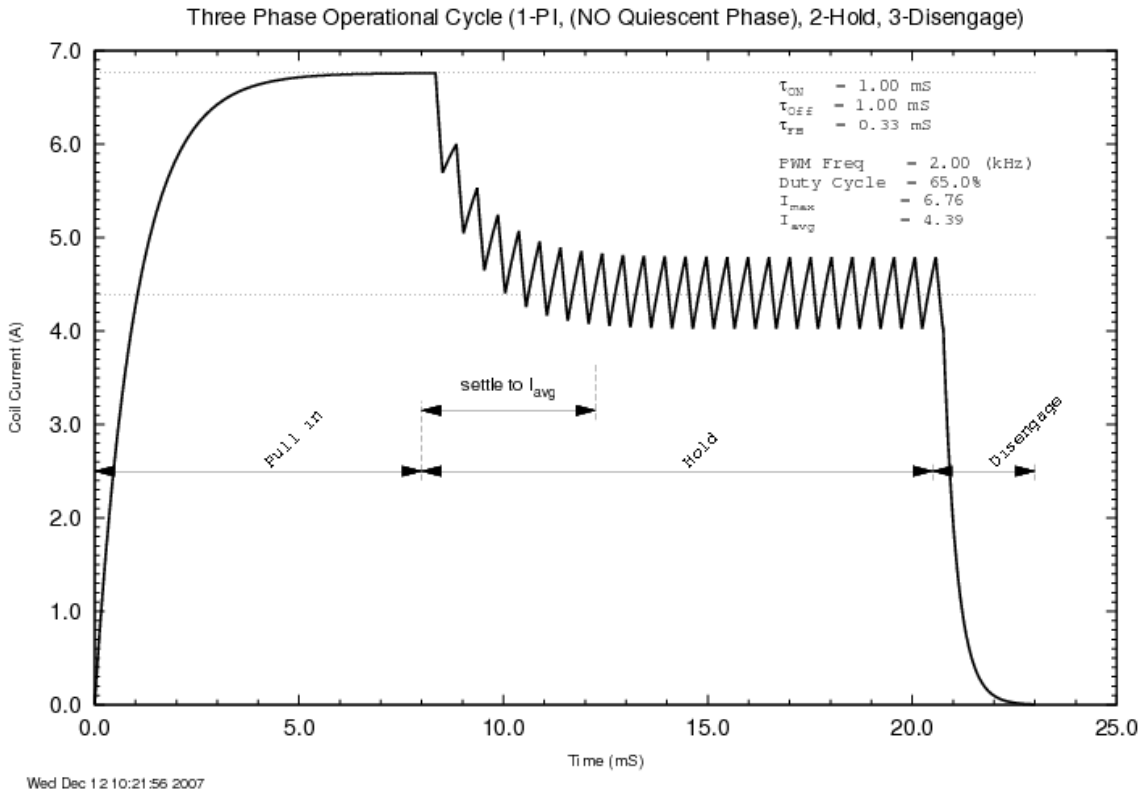

Figure 27: Ordinary Command Scheme (NO Quiescent phase)

The plot of coil current in Figure 28 is the result of a simulation that implements a four phase advanced command scheme including a Quiescent phase.

In this case, the comparison time is ~0.52mS, which is more than an **8x** improvement in transition delay (which in turn can be related to a reduction in heat dissipation). If this kind of timing is important in an application, the four phases of the advanced scheme should be utilized.

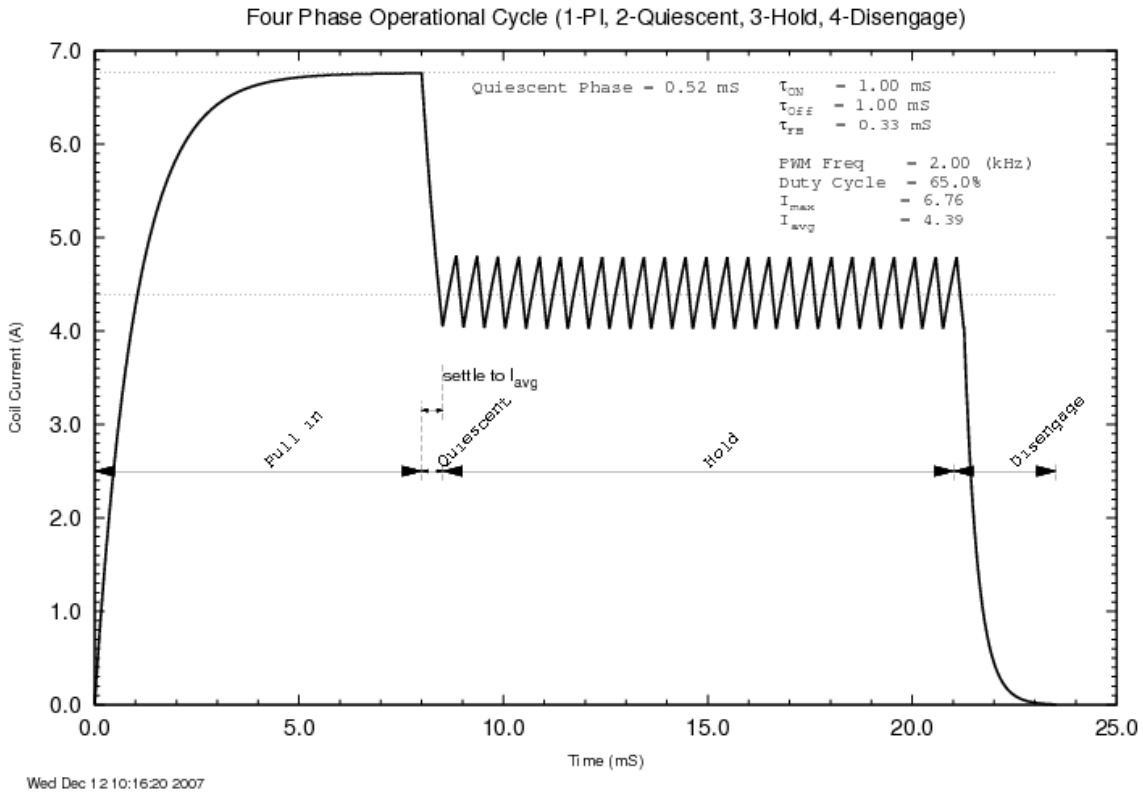

Figure 28: Advanced Command Scheme (w/ Quiescent phase)

Heat is generated within the FDMS2380 and the solenoid coil during all phases except in the disengage action phase. When the time period of the disengaged action phase is less than the thermal time constant of the installed FDMS2380, under the right ambient temperature conditions, the junction temperature will continue to increase until the device fails. In other words, it is important to not only provide adequate heat removal methods, but also to drive the device within the limits of safe operating range. The following section outlines the calculations needed to determine how much heat is generated and on which of the three pads. This information can then be used to determine the thermal design as well as the limits on operational parameters.

Thermal Calculations

The steps for a general thermal analysis are diagramed in Figure 29.

The overall thermal analysis procedure can be divided into two major interrelated sections – *SCIS*[22] *Transient* solution and *Drive & SCIS Operational Mode* solution. The following discussion will cover the Operational Mode solution with the transient solution covered in subsequent discussions.

[22] SCIS - Self Clamped Inductive Switching; see appendix "A.6: Definition of Terms and Symbols"

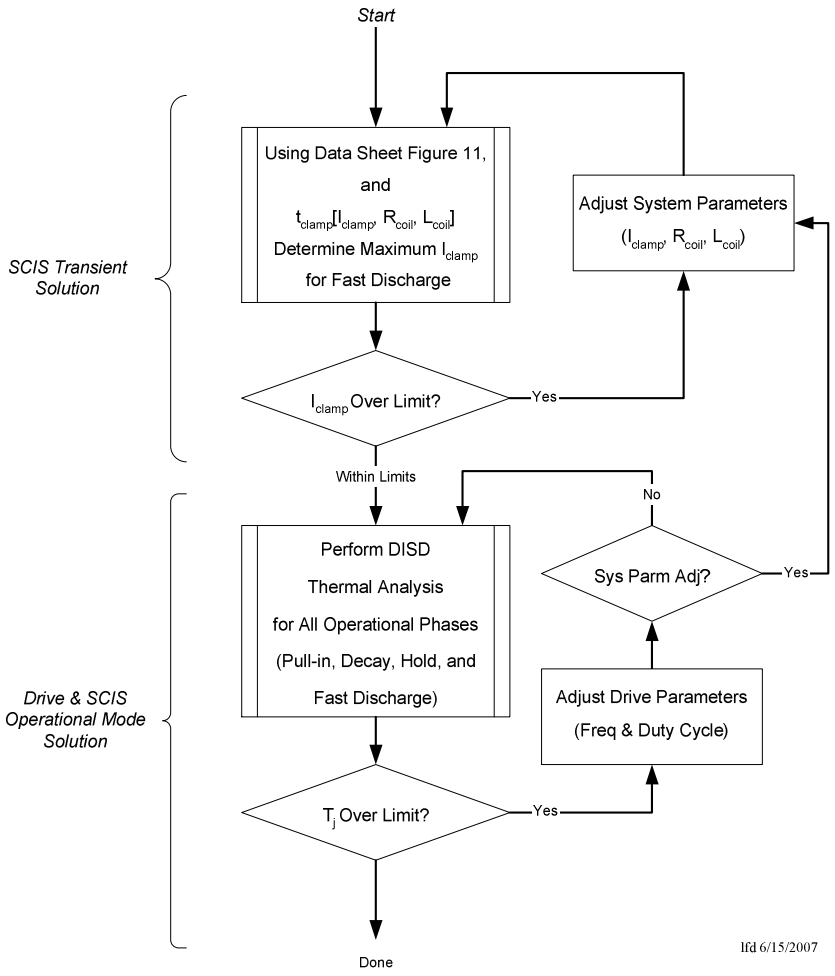

Figure 29: Steps in a General Thermal Analysis

The procedure for the operational mode solution is to determine the energy used per channel in each of the two pads (the large pad of the associated channel and small shared pad as shown in Figure 30) in all of the three FDMS2380 modes (excitation, recirculation and fast turn-off).

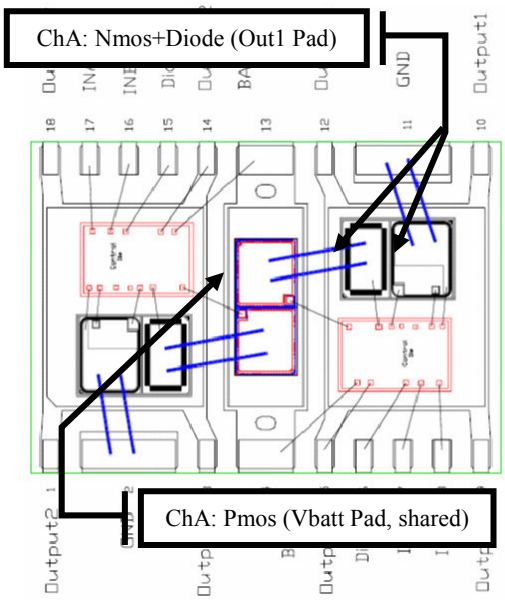

Figure 30: Layout for Multiple Die

The energies are summed together and then the duty cycle of the action command is used to determine the overall heat dissipation. The complete process is an iterative one whereby device parameters (e.g., R_{coil}, $R_{ds(on)}$, etc.) are estimated (using graphs and other data sheet information) at different temperatures as well as different operational parameters (e.g., duty cycle of action commands, etc.) and then new results are calculated.

Power is calculated based on the kind of information available as either $P=V\times I$ or $P=I^2\times R$. Energy is then calculated as power over a specific time period $\eta=P\times t$. The key elements of the circuit for these calculations are shown in Figure 31 where the output of one FDMS2380 channel is connected directly to the solenoid. Notice that the solenoid is modeled as a series combination of an inductor and a coil resistance (i.e., there are no external resistors or other components in the path). The parameter $V_{recirc(sat)}$ is obtained from the FDMS2380 data sheet while the parameter V_f is obtained from Figure 33 in this application note.

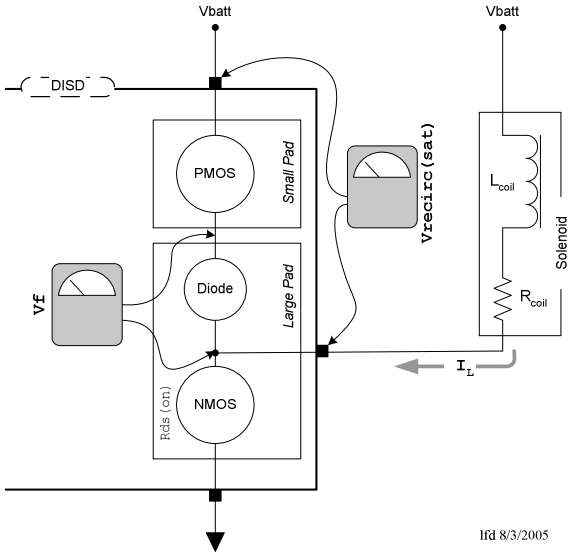

Figure 31: Circuit Elements Used for Thermal Calculations

Estimating Power Dissipation

Notice that the following calculations are based on an operation mode as depicted in Figure 25 ("*Phases of Engaging/Disengaging a Solenoid*"). Any changes to the mode of operation will require custom calculations.

Start by gathering certain basic information specified in Figure 32.

Description	*Parameter*[23]	*Value*[24]	*Units*	*Where to locate Information*
Coil inductance	L_{coil}		H	Solenoid manufacturer (open and closed)
Coil resistance	R_{coil}		Ω	Solenoid manufacturer (adjust for coil temperature)
Coil time constant	τ_{coil}		S	Calculated as: $\tau_{coil}=L_{coil}/R_{coil}$
On resistance – excitation path	$R_{ds(on)}$		Ω	FDMS2380 Data Sheet (adjust for T_j)
Saturation Voltage – Recirculation Path	$V_{Recirc(sat)}$		V	FDMS2380 Data Sheet (adjust for T_j)
Recirculation Diode Forward Voltage Drop	V_f		V	This application note (use a value from Figure 33 based on T_j)
Ambient temperature range	T_A		°C	Application requirement
Junction temperature range	T_j		°C	Application requirement
Battery Voltage	V_{batt}		V	Application requirement
Minimum Action Command Period	λ_{cmd}		S	Application requirement

[23] Parameters using λ are the period of a waveform; Parameters using a δ are 'ON' duty cycles; Parameters using a 't' are time durations

[24] Start with nominal values determined at nominal V_{batt} and nominal T_A

Description	*Parameter*[23]	*Value*[24]	*Units*	*Where to locate Information*
Action Command ON Duty Cycle	δ_A		%	Application requirement
Period of PWM	λ_{pwm}		S	Application requirement
Holding PWM ON Duty Cycle	δ_h		%	Application requirement
Duration of pull-in phase	t_{pi}		S	Application requirement
Duration of hold phase	t_{hold}		S	Application requirement
Duration of each PWM cycle when in recirculation	t_{recirc}		S	Application requirement
Estimated time in clamp	t_{clamp}		S	Application requirement
Number of time constants in pull-in	ρ	t_{pi}/τ_{coil}		Application requirement

Figure 32: Data Needed for Calculating Power

Step #1: Calculate the energy, η_{pi}, in the large pad during the pull-in phase[25]. The value η_{pi} is calculated with the average load current over the pull-in period[26], the maximum possible load current, the pull-in period and the coil time constant. It is calculated as:

Equation 15:
$$\eta_{pi} = P_{pi} \times t_{pi}$$
$$P_{pi} = I_{avgPI}^2 \times R_{ds(on)}$$
$$I_{avgPI} = I_{\max}\left[1 + \frac{1}{\rho}\left[e^{-\rho} - 1\right]\right]$$
$$I_{\max} = V_{batt} / R_{coil}$$
$$\rho = t_{pi} / \tau_{coil}$$

Step #2: Calculate the energy, η_h, in the large pad during the holding phase (PWM ON)[27] using the average current[28].

Equation 16:
$$\eta_h = N_{PWM} \times \eta_{ON}$$
$$\eta_{ON}\Big|_{per\ pwm\ event} = I_{avg(on)}^2 \times R_{ds(on)} \times t_{pwm}$$
$$I_{avg(on)} = \delta_h \times I_{\max}$$
$$t_{pwm} = \delta_h \times \lambda_{pwm}$$
$$N_{PWM} = \text{int}(t_{hold} / \lambda_{pwm})$$
$$Note\ that,$$
$$\delta_a \times \lambda_{cmd} = t_{hold} + t_{pi}$$

Step #3: Calculate the energy, η_r, in the large pad during recirculation (PWM OFF)[29] using the same average current as the PWM ON cycle[30].

Equation 17:
$$\eta_r = N_{PWM} \times \eta_{off}$$
$$\eta_{off}\Big|_{per\ pwm\ event} = V_f \times I_{recirc} \times t_{recirc}$$
$$I_{recirc} = I_{avg(on)} = \delta_h \times I_{\max}$$
$$t_{recirc} = (1 - \delta_h) \times \lambda_{pwm}$$

Step #4: Calculate the total energy in the large pad, $\eta_{total(LgPad)}$, by adding up the energy from all three operational phases. Calculate the total power in the large pad, $P_{total(LgPad)}$, as the total energy, η_{total} over the duration of the action command time, λ_{cmd}.

Equation 18: $\eta_{total(LgPad)} = \eta_{pi} + \eta_h + \eta_r$

[25] The dissipated power during the pull-in phase must NOT exceed the maximum dissipation for the large pad as specified in the data sheet.

[26] The derivation of average value for a rising exponential can be found in appendix "*A.4: Derivation for the average value of a rising and falling exponential function*"

[27] Average current, see appendix "*A.3: Determining coil current settling time, steady state coil ripple current and steady state average value for a PWM waveform driving an inductive load*"

[28] A more precise calculation could be done, if needed, by using equations from "*A.4: Derivation for the average value of a rising and falling exponential function*".

[29] See footnote #27

[30] A more precise calculation could be done, if needed, by using equations from "*A.4: Derivation for the average value of a rising and falling exponential function*".

Equation 19: $P_{total(LgPad)} = \frac{\eta_{total(LgPad)}}{\lambda_{cmd}}$

Step #5: Calculate the energy in part of the center pad (the portion occupied by only the selected channels PMOS PowerFET) during recirculation[31], again using the average PWM ON current[32].

Equation 20: $\eta_{rsp} = N_{PWM} \times \eta_{rspEVT}$

$Where:$

$$\eta_{rspEVT}\Big|_{per\ \ pwm\ \ event} = (V_{recirc(sat)} - V_f) \times I_{recirc} \times t_{recirc}$$

$$I_{recirc} = I_{avg(on)} = \delta_h \times I_{\max}$$

$$t_{recirc} = (1 - \delta_h) \times \lambda_{pwm}$$

Step #6: Calculate the energy stored in the magnetic field[33] during fly-back for the average holding current.

Equation 21: $\eta_{fb} = \frac{1}{2} I_{avg}^2 \times L$

$$I_{avg} = \delta_h \times I_{\max}$$

Given that[34]:

Equation 22: $(1 - \delta_a) \times \lambda_{cmd} > t_{clamp}$

$$Where: \quad t_{clamp} = \tau \log_e \left(1 + \frac{R_{coil}}{V_{clamp} / I_{clamp}} \right)$$

This requirement necessitates that all the magnetic energy be removed from the coil before starting the next action command.

Step #7: Calculate the total energy for the half of the small pad and the resulting power dissipation.

Equation 23: $\eta_{total(SmPad)} = \eta_{rsp} + \eta_{fb}$

Equation 24: $P_{total(SmPad)} = \frac{\eta_{total(SmPad)}}{\lambda_{cmd}}$

Equation 25: $P_{total(chan)} = P_{total(smPad)} + P_{total(LgPad)}$

Step #8: Repeat steps #1 to #7 for the alternate channel to get $P2_{total(LgPad)}$ and $P2_{total(SmPad)}$.

The thermal performance of the device in a particular application can be determined once the calculations outlined above are completed for both channels (step #1 through step #8). The resultant power values are then used in the thermal calculations outlined in the next chapter.

It is critical to remember that these calculations must be done in an iterative fashion so that temperature sensitive device parameters (e.g. $R_{ds(on)}$ as used in Equation 16, etc.) can be adjusted for each iteration to reflect changes in the junction temperature. In most cases, it will only take a few iterations for the results to stabilize.

[31] The initials "rsp" mean Recirculation Small Pad; Flyback dissipation in the diode alone, located on the large pad, is accounted for in a previous step

[32] A more precise calculation could be done, if needed, by using equations from "*A.4: Derivation for the average value of a rising and falling exponential function*".

[33] In general, inductance (L, with units Henry's which are defined as webers/amp meaning flux per unit current) is not a constant and when the coil current increase so that the solenoid core nears magnetic saturation, L becomes significantly smaller with higher coil currents. Therefore, the energy stored in the magnetic field increases at a lower rate then when the core is NOT saturated (i.e., the energy stored in the magnetic field when the core is saturated is not equal to $\frac{1}{2} L I^2$).

[34] For derivation see "A.5: Derivation of Time in Clamp Equation" on page 53

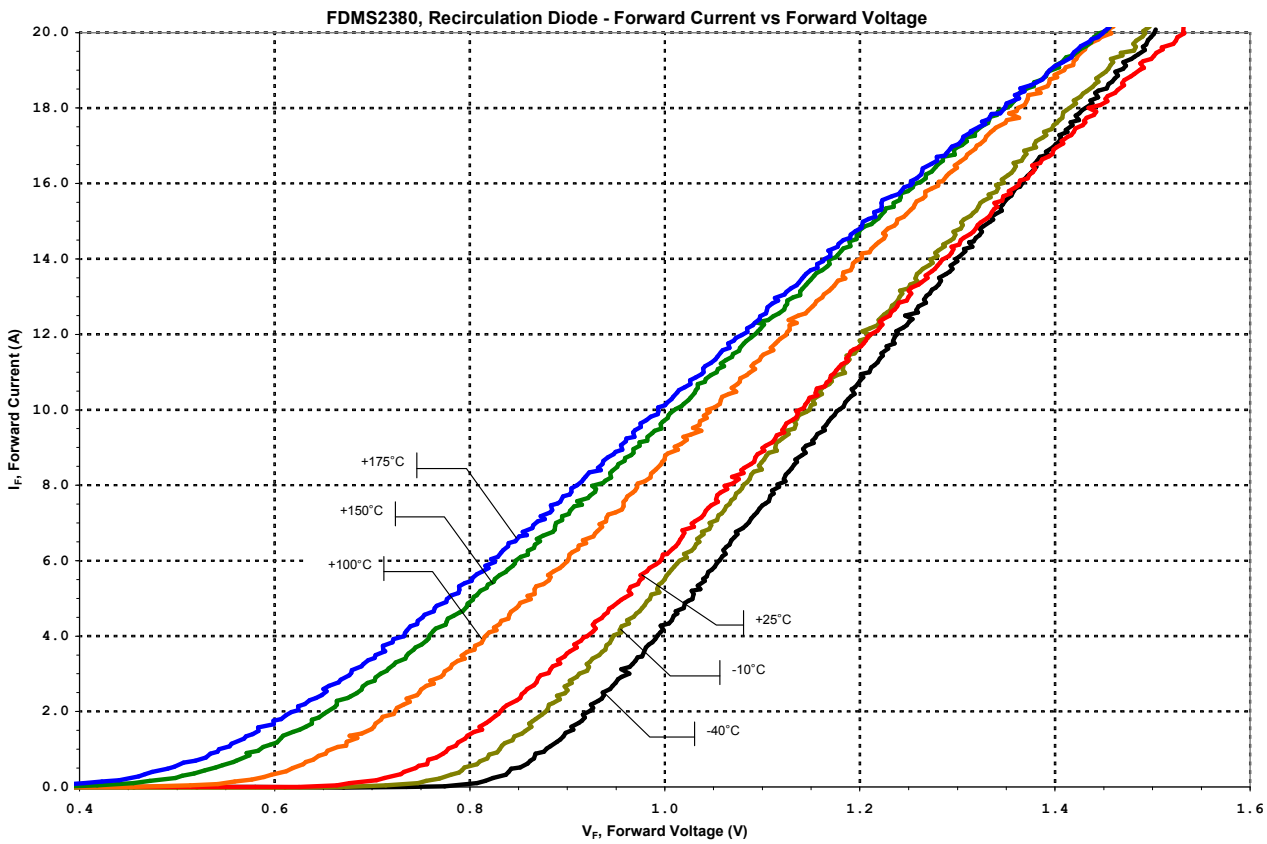

Figure 33: FDMS2380 Forward-Biased Characteristics of the Internal Recirculation Diode

The results of all the calculations can be summarized and placed in the appropriate cell in a table like that of Figure 34 for use in the next chapter on thermal analysis.

FDMS2380 Power Dissipation	*Power Dissipation*
Large pad (1st Channel)	
Large pad (2nd Channel)	
Small pad	
Small pad (1st Channel) Small pad (2nd Channel)	
Total Dissipation	

Figure 34: Summary of Calculation Results Form

A complete example of a thermal analysis is explored in the section titled "*Example Thermal Analysis*" starting on page 27.

External voltages and currents for a typical cycle of device operation are shown in the screen capture of Figure 35. The four traces, for one select channel, are:

1. Voltage at the pin: `In A`
2. Voltage at the pin: `In B`
3. Current through the pin: `Out`
4. Voltage at the pin: `Out`

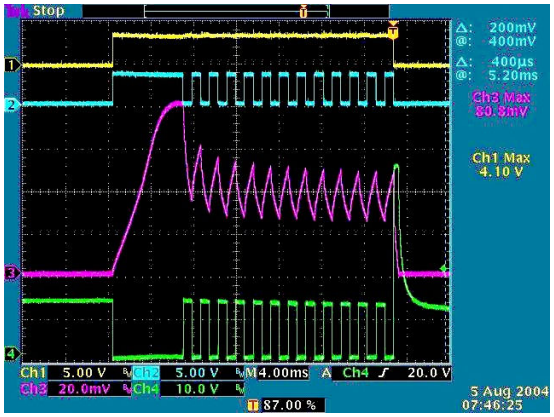

Figure 35: DSO Screen Capture

The pull-in phase is identified by finding the first low to high transition of the `In A` signal (trace #2) through the first high to low transition of the signal. Examining the output current (trace #3) during the pull-in phase shows that the pull-in period is long enough in duration that the coil current rises to the maximum value before the holding phase begins. The start of the fly-back phase is identified by the high to low transition of the `In A` signal (trace #1). The output voltage (trace #4) correspondingly rises quickly and begins to decay as the stored energy is drained out of the magnetic field of the solenoid coil.

Estimating Maximum Junction Temperature

Estimating junction temperature can be done statically (i.e., steady state conditions) and dynamically (i.e., based on transient operating conditions). A simplified thermal model is represented in Figure 36 as an electrical equivalent where heat flow is analogous to electric current and temperature corresponds to voltage.

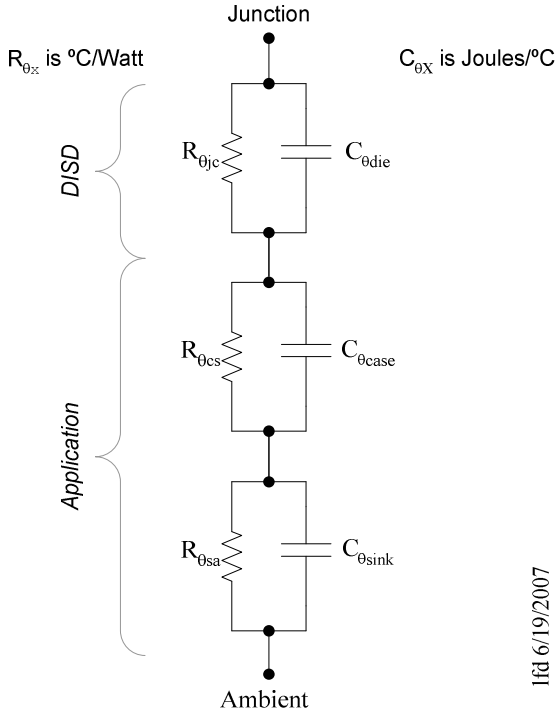

Figure 36: Simplified Thermal Model

As heat is applied to an object, such as an aluminum heat sink or a silicon die, its temperature rises slowly. This is analogous to current flowing into a capacitor followed by the voltage across the capacitor correspondingly increasing. The amount of heat applied and the thermal time constant determines how fast the temperature rises.

To simplify the calculations, only the static case will be considered here (the static case is typically sufficient for most solenoid applications). Then in this particular case, the capacitors shown in Figure 36 can be eliminated.

The equation used to find the junction temperature (T_J) is as follows:

Equation 26

$$T_j = T_A + R_{\theta JA} \times P$$

$$R_{\theta JA} = R_{\theta JC} + R_{\theta CS} + R_{\theta SA}$$

Where: T_A is the ambient temperature

$R_{\theta JA}$ is the thermal resistance - junction to ambient[35]

P is the device power dissipation

$R_{\theta JC}$ is the thermal resistance – junction to case

$R_{\theta CS}$ is thermal resistance – case to heat-sink

$R_{\theta CA}$ is thermal resistance – heat-sink to ambient

The value for $R_{\theta JC}$ can be found in the FDMS2380 data sheet, while the other thermal resistances are application dependant. The latest FDMS2380 data sheet should be consulted, but for this discussion, an $R_{\theta JC}$ value of 3.5°C/W will be used for each of the two large pads and 4.0°C/W for the small pad. The challenge for developing a thermally efficient system is that the mechanical connection between a FDMS2380 pad and its heat-sink must also be an electrical insulator. The two large pads and one small FDMS2380 pad must be electrically insulated from the heat sink because of potential EMI problems and to guard against fault conditions where the pad develops a low impedance path to ground. Further thermal design challenges arise from the smaller pad (internally attached to the Pmos device) having a smaller footprint for heat flow. In general, the following categorizes values for $R_{\theta CA}$:

- Very good ≤ 6.0 to 20.0°C/W
- Typical 30.0 to 40.0°C/W
- Poor ≥ 70.0°C/W

The final part of the thermal analysis is to use the power values for each of the three pads (determined in the previous chapter) and, using appropriate thermal resistances, calculate the junction temperature (using the equation above). Next, verify that the maximum junction temperature (from the latest data sheet) is not exceeded (using a reasonable margin of safety, say 20%). A safety margin is used to account for inexactness in the simplified model and other inaccuracies in the data used.

Example Thermal Analysis

The following pages are a complete example of a thermal analysis done in MathCAD® in such a way that the intermediate numerical results are shown to simplify the understanding of the calculations.

Make notice that the temperature sensitive parameter values for $R_{ds(on)}$ come from the FDMS2380 data sheet, while the values for V_f come from this application note (see Figure 33 found on page 26).

[35] Notice that the data sheet gives a trial value for $R_{\theta JA}$ in the *Thermal Characteristics* section, but it is for a specific heat sink of one square inch of PWB copper (with other parameters specified), this data sheet value is to be used only for system comparison purposes.

Example 1: Energy, Power and Heat Calculations

L. F. Durfee; Rev A Released: 06Jul2007

Application Parameters[36]*:*

$V_{batt} := 14$ $R_{coil} := 0.91$ $L_{coil} := 1.29 \cdot 10^{-3}$ $R_{ds\_on\_NMOS} := 30.0 \cdot 10^{-3}$ $V_f := 0.90$ $T_j := 25.0$

$L_{coil\_Closed} := 1.54 \cdot 10^{-3}$ $V_{recirc\_sat} := 1.10$

$\lambda_{cmd} := 50 \cdot 10^{-3}$ $t_{pi} := 14.18 \cdot 10^{-3}$ $t_{hold} := 5.82 \cdot 10^{-3}$ $\lambda_{pwm} := 200 \cdot 10^{-6}$ $\delta_{h\_ON} := 0.60$

$R_{\theta jc\_Lg} := 3.5$ $T_{amb} := 25.0$

$R_{\theta jc\_sm} := 4.0$ $R_{\theta CA} := 30.0$

$f_{cmd} := \frac{1}{\lambda_{cmd}} \rightarrow \frac{1}{50 \cdot 10^{-3}}$ $f_{cmd} = 20.000$

$I_{max} := \frac{V_{batt}}{R_{coil}} \rightarrow \frac{14}{0.91} = 15.385$ $\tau_{coil} := \frac{L_{coil}}{R_{coil}} \rightarrow \frac{1.29 \cdot 10^{-3}}{0.91} = 1.418 \times 10^{-3}$ $\rho := \frac{t_{pi}}{\tau_{coil}} \rightarrow \frac{14.18 \cdot 10^{-3}}{\frac{1.29 \cdot 10^{-3}}{0.91}} = 10.003$

$I_{max} = 15.385$ $\tau_{coil} = 1.418 \times 10^{-3}$ $\rho = 10.003$

Voltage in Volts
Current in Amps
Resistance in Ohms
Inductance in Henries
Temperature in Degrees Celsius
Time in Seconds
Time Constants in Seconds
Duty Cycle in fractions 0 to 1
Energy in Joules
Power in Watts

λ is a Duration (in Seconds)
δ is a Duty Cycle (fraction from 0 to 1)
τ is a Time Constant (in Seconds)
ρ is a Ratio (dimensionless)
η is Energy (in Joules)
t is a Time Duration (in Seconds)
T is a Temperature (in degrees Celsius)
R is Resistance (in Ohms)
V is Voltage (in Volts)
I is Current (in Amperes)
P is Power (in Watts)
f is Frequency (in Hertz)

[36] Please read the comments at the end of this section (on page 35)

Step #1: Calculate Pull-In Energy, η_{pi}

$V_{batt} = 14.000$ $R_{coil} = 910.000\times 10^{-3}$ $L_{coil} = 1.290\times 10^{-3}$ $t_{pi} = 14.180\times 10^{-3}$ $R_{ds\_on\_NMOS} = 30.000\times 10^{-3}$

$I_{max} = 15.385$ $\tau_{coil} = 1.418\times 10^{-3}$ $\rho = 10.003$

$$I_{avgPI} := I_{max}\cdot\left[1+\frac{1}{\rho}\left(e^{-\rho}-1\right)\right] \rightarrow \frac{14}{0.91}\cdot\left[1+\frac{1}{\frac{14.18\cdot 10^{-3}}{\frac{1.29\cdot 10^{-3}}{0.91}}}\cdot\left(e^{-\frac{14.18\cdot 10^{-3}}{\frac{1.29\cdot 10^{-3}}{0.91}}}-1\right)\right]$$

$$I_{avgPI} = 13.847$$

$$\eta_{pi} := I_{avgPI}^{2}\cdot R_{ds\_on\_NMOS}\cdot t_{pi} \rightarrow \left[\frac{14}{0.91}\cdot\left[1+\frac{1}{\frac{14.18\cdot 10^{-3}}{\frac{1.29\cdot 10^{-3}}{0.91}}}\cdot\left(e^{-\frac{14.18\cdot 10^{-3}}{\frac{1.29\cdot 10^{-3}}{0.91}}}-1\right)\right]\right]^{2}\cdot 30.0\cdot 10^{-3}\cdot 14.18\cdot 10^{-3}$$

$$\eta_{pi} = 81.562\times 10^{-3}$$

Step #2: Calculate Energy in Holding Phase, η_h

$t_{hold} = 5.820\times 10^{-3}$ $\lambda_{pwm} = 200.000\times 10^{-6}$ $\delta_{h\_ON} = 600.000\times 10^{-3}$ $R_{ds\_on\_NMOS} = 30.000\times 10^{-3}$

$$N_{pwm} := \text{trunc}\left(\frac{t_{hold}}{\lambda_{pwm}}\right) \rightarrow \text{trunc}\left(\frac{5.82\cdot 10^{-3}}{200\cdot 10^{-6}}\right)$$

$N_{pwm} = 29.000$

$$t_{pwm\_on} := \delta_{h\_ON}\cdot\lambda_{pwm} \rightarrow 0.60\cdot 200\cdot 10^{-6}$$

$t_{pwm\_on} = 120.000\times 10^{-6}$

$$I_{avg} := \delta_{h\_ON}\cdot I_{max} \rightarrow 0.60\cdot\frac{14}{0.91}$$

$I_{avg} = 9.231$

$$\eta_{ON\_per} := I_{avg}^{2}\cdot R_{ds\_on\_NMOS}\cdot t_{pwm\_on} \rightarrow \left(0.60\cdot\frac{14}{0.91}\right)^{2}\cdot 30.0\cdot 10^{-3}\cdot 0.60\cdot 200\cdot 10^{-6}$$

$\eta_{ON\_per} = 306.746\times 10^{-6}$

$$\eta_h := N_{pwm}\cdot\eta_{ON\_per} \rightarrow \text{trunc}\left(\frac{5.82\cdot 10^{-3}}{200\cdot 10^{-6}}\right)\cdot\left(0.60\cdot\frac{14}{0.91}\right)^{2}\cdot 30.0\cdot 10^{-3}\cdot 0.60\cdot 200\cdot 10^{-6}$$

$\boxed{\eta_h = 8.896\times 10^{-3}}$

Step #3: Calculate Energy in Large Pad During Recirculation Phase, η_r

$$t_{recirc} := \left(1 - \delta_{h\_ON}\right) \cdot \lambda_{pwm} \rightarrow (1 - 0.60) \cdot 200 \cdot 10^{-6}$$

$$t_{recirc} = 80.000 \times 10^{-6}$$

$$I_{recirc} := \delta_{h\_ON} \cdot I_{max} \rightarrow 0.60 \cdot \frac{14}{0.91}$$

$$I_{recirc} = 9.231$$

$$\eta_{off\_per} := V_f \, I_{recirc} \cdot t_{recirc} \rightarrow 0.90 \cdot 0.60 \cdot \frac{14}{0.91} \cdot (1 - 0.60) \cdot 200 \cdot 10^{-6}$$

$$\eta_{off\_per} = 664.615 \times 10^{-6}$$

$$\eta_r := N_{pwm} \cdot \eta_{off\_per} \rightarrow \text{trunc}\left(\frac{5.82 \cdot 10^{-3}}{200 \cdot 10^{-6}}\right) \cdot 0.90 \cdot 0.60 \cdot \frac{14}{0.91} \cdot (1 - 0.60) \cdot 200 \cdot 10^{-6}$$

$$\boxed{\eta_r = 19.274 \times 10^{-3}}$$

Step #4: Calculate Total Energy in Large Pad, $\eta_{total(LgPad)}$, and Total power, $P_{total(LgPad)}$

$\eta_{pi} = 81.562\times 10^{-3}$ $\eta_{h} = 8.896\times 10^{-3}$ $\eta_{r} = 19.274\times 10^{-3}$ $\lambda_{cmd} = 50.000\times 10^{-3}$

$$\eta_{total\_LgPad} := \eta_{pi} + \eta_{h} + \eta_{r}$$

$$\eta_{total\_LgPad} = 109.732\times 10^{-3}$$

$$P_{total\_LgPad} := \frac{\eta_{total\_LgPad}}{\lambda_{cmd}}$$

$$\boxed{P_{total\_LgPad} = 2.195}$$

Step #5: Calculate Energy in PMOS During Recirculation in <u>Small Pad</u>, η_{rsp}

$$\eta_{pmos\_per} := \left(V_{recirc\_sat} - V_{f}\right)\cdot I_{avg}\cdot t_{recirc} \rightarrow (1.10 - 0.90)\cdot 0.60\cdot\frac{14}{0.91}\cdot(1 - 0.60)\cdot 200\cdot 10^{-6}$$

$$\eta_{pmos\_per} = 147.692\times 10^{-6}$$

$$\eta_{rsp} := \eta_{pmos\_per}\cdot N_{pwm} \rightarrow (1.10 - 0.90)\cdot 0.60\cdot\frac{14}{0.91}\cdot(1 - 0.60)\cdot 200\cdot 10^{-6}\cdot\text{trunc}\left(\frac{5.82\cdot 10^{-3}}{200\cdot 10^{-6}}\right)$$

$$\boxed{\eta_{rsp} = 4.283\times 10^{-3}}$$

Step #6: Calculate Energy Stored in Magnetic Field (dissipated by PMOS)[37], η_{fb}

$$\eta_{fb} := \frac{1}{2}\cdot I_{avg}{}^{2}\cdot L_{coil\_Closed} \rightarrow \frac{1}{2}\cdot\left(0.60\cdot\frac{14}{0.91}\right)^{2}\cdot 1.54\cdot 10^{-3}$$

$$\eta_{fb} = 65.609\times 10^{-3}$$

Step #7: Calculate Total Energy for Small Pad, η_{total_smPad}, Resulting Power Dissipation and Total Channel Power

$\eta_{rsp} = 4.283\times 10^{-3}$ $\eta_{fb} = 65.609\times 10^{-3}$ $P_{total\_LgPad} = 2.195$

$$\eta_{total\_smPad} := \eta_{rsp} + \eta_{fb}$$

$$\eta_{total\_smPad} = 69.893\times 10^{-3}$$

$$P_{total\_smPad} := \frac{\eta_{total\_smPad}}{\lambda_{cmd}}$$

$$P_{total\_smPad} = 1.398$$

$$P_{total\_Chan} := P_{total\_LgPad} + P_{total\_smPad}$$

$$P_{total\_Chan} = 3.592$$

[37] Notice that this is a worst case calculation by using L_{coil_Closed}

Final Step: Calculate T_j Rise Given Power Dissipation

$R_{\theta jc\_Lg} = 3.500$ $R_{\theta jc\_sm} = 4.000$ $R_{\theta CA} = 30.000$ $T_{amb} = 25.000$

$P_{total\_LgPad} = 2.195$ $P_{total\_smPad} = 1.398$

$$T_{NMOS} := T_{amb} + P_{total\_LgPad} \cdot \left(R_{\theta jc\_Lg} + R_{\theta CA}\right)$$

$$T_{NMOS} = 98.520$$

$$T_{PMOS} := T_{amb} + P_{total\_smPad} \cdot \left(R_{\theta jc\_sm} + R_{\theta CA}\right)$$

$$T_{PMOS} = 72.527$$

Notice, for example, that $R_{ds(on)}$ at 25°C is 30mΩ (as used in these calculations), while $R_{ds(on)}$ at 150°C is 50mΩ, which is a 67% increase. So, as mentioned earlier, this analysis would be repeated by multiple updates of each temperature dependent variable (e.g., $R_{ds(on)}$, V_f, etc.) until the results stabilize (typically 2 or 3 iterations are needed). Furthermore, notice that the initial calculation for coil current exceeds the minimum $I_{out(trip)}$ value (even at 25°C) and therefore the system parameters need to be modified before this example can be used in an application.

Flyback Considerations

When the application needs to deactivated the solenoid quickly, the FDMS2380 can be commanded into fast turn-off mode by setting InA=InB="0". The coil current will then ramp down at the fastest possible rate. This fast turn-off mode puts the PMOS device into an active state that clamps the output voltage to a maximum value (data sheet parameter $V_{out(cl2)}$). This fast turn-off scheme is called Self Clamped Inductive Switching or SCIS. A simplified simulation circuit to illustrate the clamped mode is shown in Figure 37.

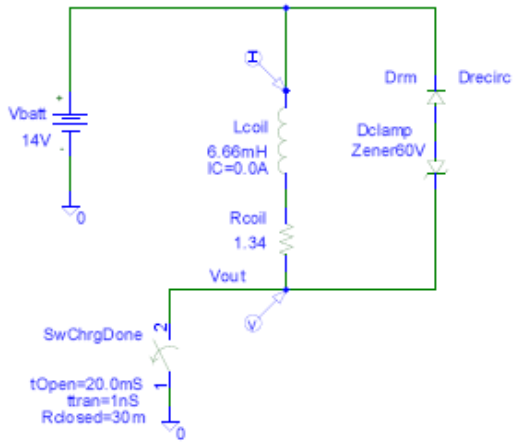

Figure 37: Simple Clamp Circuit Simulation

The simulated output is shown in Figure 38.

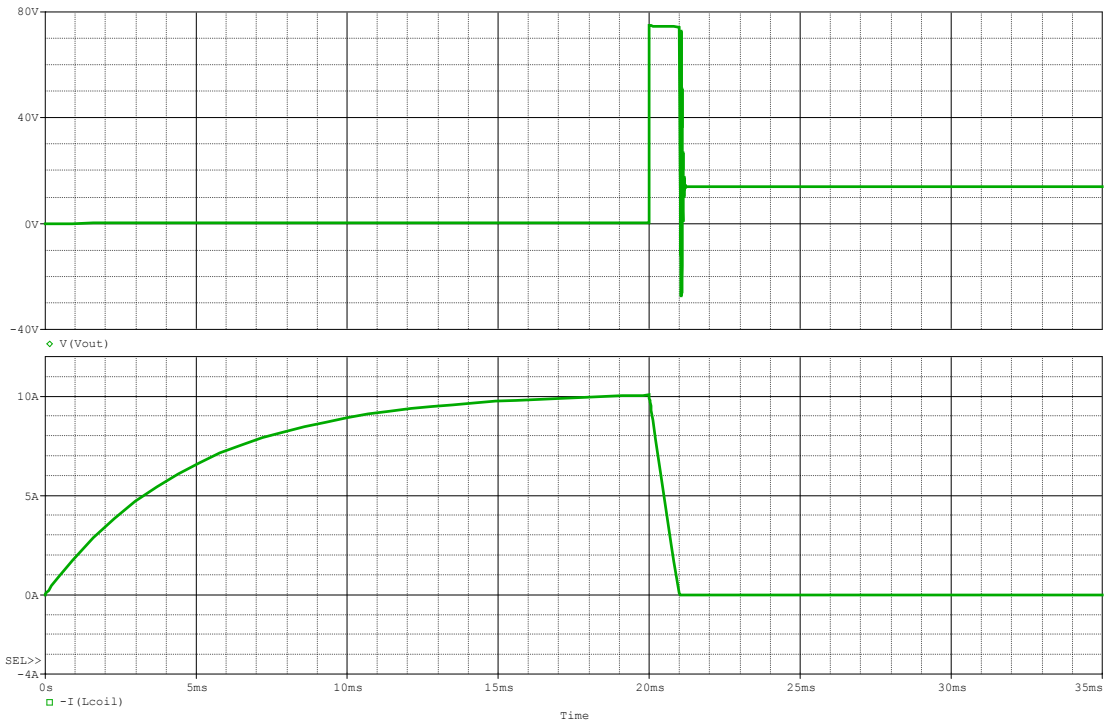

Figure 38: Fast Turn-off Clamp Simulation

Looking at the results of the simulation, the fast turn-off mode starts at time 20mS (after the solenoid is fully charged) and the coil current is then reduced to zero (0) at about 21mS. That is, going from a fully charged solenoid to a fully discharged solenoid can be accomplished in ~1mS.

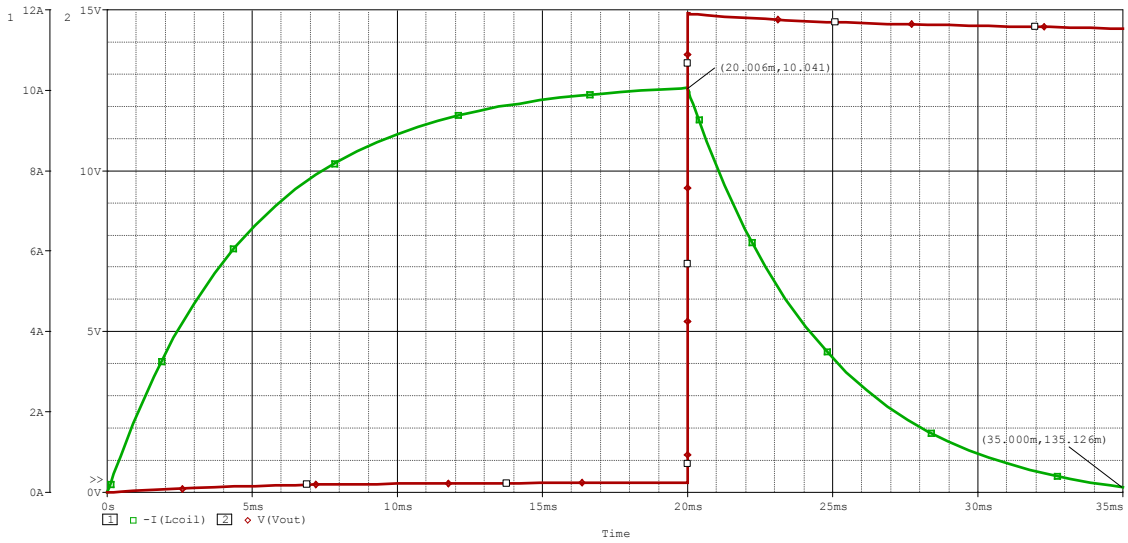

Figure 39: Simulation of Current Decay by Shorting-out the Coil

Another scheme to discharge the energy in the coil is to simply short the two ends of the coil together. The simulation results, using the same parameters as the last simulation, are shown in Figure 39. In this case, the simulation shows that the duration required to bring the current to zero (0) is more than 15mS (from 20mS to over 35mS in the simulation), which is considerably longer (over **15:1** longer) than the duration for the voltage clamp scheme.

The dissipation of energy in the PMOS device during fast turn-off must be maintained within the capabilities of the device, and all applications must guard against overstress. The photograph in Figure 40 is a magnified view of a PMOS die that shows the results of overstressing the SCIS (Self Clamped Inductive Switching) capabilities of a FDMS2380.

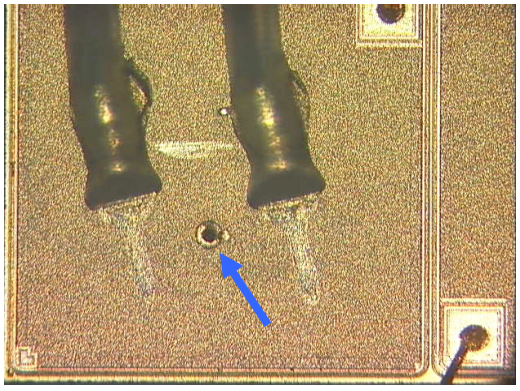

Figure 40: An Electrical Over Stress (EOS) failure on the PDMOS die

The arrow points to the damaged PMOS die area, which is a source to drain direct short, resulting in, for this case, a non-functional FDMS2380.

There are several graphs in the data sheet which allow a variety of ways to modify the application to prevent device SCIS overstress.

The following discussion uses the *Time in Clamp* graph and method to keep the FDMS2380 within safe limits. The procedure is to adjust system parameters (e.g., coil inductance, current flow at start of fast shut-down, etc.), as needed to meet time in clamp SCIS safety conditions (from the data sheet graph). The parameters and there interrelations are shown in Figure 41.

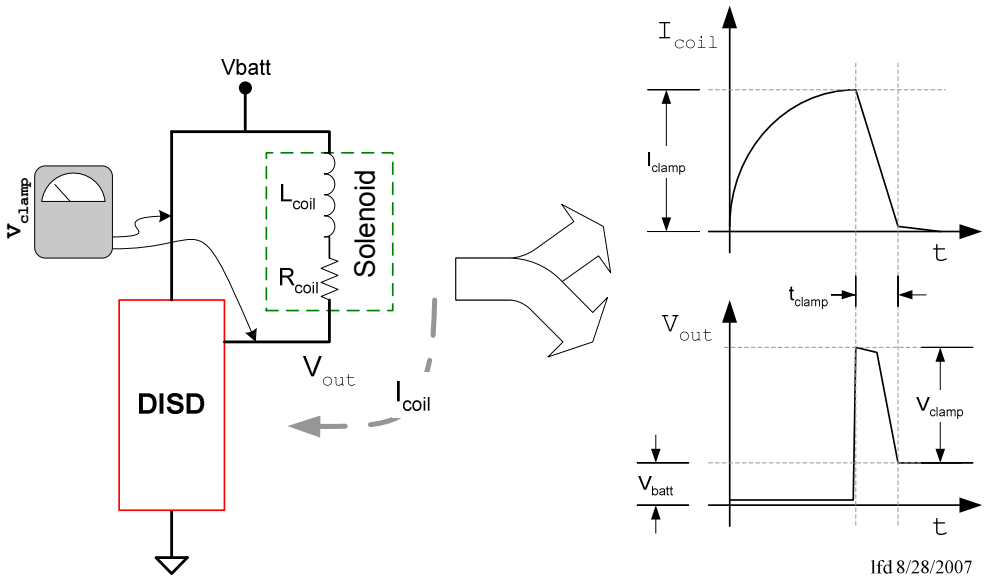

Figure 41: Time in Clamp Circuit and Parameters

The upper right hand plot in the figure shows that I_{clamp} is the coil current magnitude just prior to going into fast-shutdown mode. It shows that the clamp voltage, V_{clamp}, is measured on top of V_{batt}. It further shows that the time in clamp, t_{clamp}, is measured from the time when the fast turn-off mode is commanded and continues until the coil current drops to near zero.

The equation that predicts[38] the time in clamp[39] is:

Equation 27

$$t_{clamp} = \tau \log_e \left(1 + \frac{R_{coil}}{V_{clamp} / I_{clamp}} \right)$$

Where: $$I_{clamp} = \frac{\delta \bullet V_{batt}}{R_{coil} + R_{ds(on)}}$$

$$\tau = \frac{L_{coil}}{R_{coil}}$$

Since $R_{coil} >> R_{ds(on)}$, the NMOS $R_{ds(on)}$ can be ignored with little loss in accuracy. The parameter δ can be varied as $0.0 < \delta \leq 1.0$ to adjust the amount of current flowing before fast turn-off mode is entered.

The following is an example SCIS calculation. The example was done in MathCAD® in such a way that the intermediate numerical results are shown to simplify the understanding of the calculations.

Notice that there are four (4) cases – two for the inductance of the plunger within the “out” position range and two for the plunger within the “in” position range. The inductance value is different for each of these two mechanical positions (which is a consideration for all applications). Notice that the inductances increases when the solenoid is within the “in” positions range (for this particular arrangement). Each of these cases are further divided into two cases where the first is a calculation of full current and the next is the calculation for a coil current value that keeps the FDMS2380 within a safe SCIS operating point.

These example calculations clearly show the need to evaluate the FDMS2380 using a wide range of operational parameters to insure it is run within its safe limits.

Notice also, that this is only one of many ways available to ensure that the application is SCIS safe. That is, the data sheet has other related information that could be used for the analysis.

[38] Consider the assumptions and limitations as stated in the derivation found in Appendix “*A.5: Derivation of Time in Clamp Equation*”

[39] The derivation can be found in Appendix “*A.5: Derivation of Time in Clamp Equation*”

SCIS Calculations for the FDMS2380 (DISD)

$R_{ds\_ON} := 30 \cdot 10^{-3}$ $V_{clamp} := 30.00$ $V_{batt} := 14.00$ $R_{coil} := 0.910$

$$I_{max} := \frac{V_{batt}}{R_{coil}} \rightarrow \frac{14.00}{0.910} \qquad I_{max} = 15.385 \times 10^{0}$$

Case I: Plunger Out, high duty cycle

$L_{coil} := 1.29 \cdot 10^{-3}$ $\delta_{pwm\_ON} := 0.98$

$$\tau := \frac{L_{coil}}{R_{coil}} \rightarrow \frac{1.29 \cdot 10^{-3}}{0.910}$$

$$\tau = 1.418 \times 10^{-3}$$

$$I_{clamp} := \delta_{pwm\_ON} \cdot I_{max} \rightarrow 0.98 \cdot \frac{14.00}{0.910}$$

$$I_{clamp} = 15.077 \times 10^{0}$$

$$t_{clamp} := \tau \cdot \ln\left[1 + \left(\frac{R_{coil}}{\frac{V_{clamp}}{I_{clamp}}}\right)\right] \rightarrow \frac{1.29 \cdot 10^{-3}}{0.910} \cdot \ln\left(1 + \frac{0.910}{\frac{30.00}{0.98 \cdot \frac{14.00}{0.910}}}\right)$$

$$t_{clamp} = 533.873 \times 10^{-6}$$

SCIS damage would result! Based on the FDMS2380 data sheet figure 11, an I_{clamp} of 15 Amps, allows a maximum time in clamp of ~250uS (at 25degC).

Case II: Plunger Out, SCIS safe duty cycle

$\delta_{pwm\_ON} := 0.65$

$$\tau := \frac{L_{coil}}{R_{coil}} \rightarrow \frac{1.29 \cdot 10^{-3}}{0.910}$$

$$\tau = 1.418 \times 10^{-3}$$

$$I_{clamp} := \delta_{pwm\_ON} \cdot I_{max} \rightarrow 0.65 \cdot \frac{14.00}{0.910}$$

$$I_{clamp} = 10.000 \times 10^{0}$$

$$t_{clamp} := \tau \cdot \ln\left[1 + \left(\frac{R_{coil}}{\frac{V_{clamp}}{I_{clamp}}}\right)\right] \rightarrow \frac{1.29 \cdot 10^{-3}}{0.910} \cdot \ln\left(1 + \frac{0.910}{\frac{30.00}{0.65 \cdot \frac{14.00}{0.910}}}\right)$$

$$t_{clamp} = 375.553 \times 10^{-6}$$

Works! *Based on the FDMS2380 data sheet figure 11, an I_{clamp} of 10 Amps, allows a maximum time in clamp of ~400uS (at 25degC).*

It should be noted that calculations need to be done at temperature extremes as well.

$$I_{max} := \frac{V_{batt}}{R_{coil}} \rightarrow \frac{14.00}{0.910} \qquad I_{max} = 15.385 \times 10^{0}$$

Case III: Plunger IN, high duty cycle (I_{coil} changes)

$$L_{coil} := 1.54 \cdot 10^{-3} \qquad \delta_{pwm\_ON} := 0.98$$

$$\tau := \frac{L_{coil}}{R_{coil}} \rightarrow \frac{1.54 \cdot 10^{-3}}{0.910}$$

$$\tau = 1.692 \times 10^{-3}$$

$$I_{clamp} := \delta_{pwm\_ON} \cdot I_{max} \rightarrow 0.98 \cdot \frac{14.00}{0.910}$$

$$I_{clamp} = 15.077 \times 10^{0}$$

$$t_{clamp} := \tau \cdot \ln\left[1 + \left(\frac{R_{coil}}{\frac{V_{clamp}}{I_{clamp}}}\right)\right] \rightarrow \frac{1.54 \cdot 10^{-3}}{0.910} \cdot \ln\left(1 + \frac{0.910}{\frac{30.00}{0.98 \cdot \frac{14.00}{0.910}}}\right)$$

$$t_{clamp} = 637.337 \times 10^{-6}$$

SCIS damage would result! Based on the FDMS2380 data sheet figure 11, an I_{clamp} of 15 Amps, allows a maximum time in clamp of ~250uS (at 25degC).

Case IV: Plunger IN, SCIS safe duty cycle

$$\delta_{pwm\_ON} := 0.60$$

$$\tau := \frac{L_{coil}}{R_{coil}} \rightarrow \frac{1.54 \cdot 10^{-3}}{0.910}$$

$$\tau = 1.692 \times 10^{-3}$$

$$I_{clamp} := \delta_{pwm\_ON} \cdot I_{max} \rightarrow 0.60 \cdot \frac{14.00}{0.910}$$

$$I_{clamp} = 9.231 \times 10^{0}$$

$$t_{clamp} := \tau \cdot \ln\left[1 + \left(\frac{R_{coil}}{\frac{V_{clamp}}{I_{clamp}}}\right)\right] \rightarrow \frac{1.54 \cdot 10^{-3}}{0.910} \cdot \ln\left(1 + \frac{0.910}{\frac{30.00}{0.60 \cdot \frac{14.00}{0.910}}}\right)$$

$$t_{clamp} = 417.763 \times 10^{-6}$$

Works! *Based on the FDMS2380 data sheet figure 11, an I_{clamp} of 9.2 Amps, allows a maximum time in clamp of ~425uS (at 25degC).*

Solenoid Current Ripple

As the PWM signal on InB turns on and turns off, during the hold phase, the solenoid current will correspondingly rise and fall. This ripple in current will cause a ripple in applied force to the solenoid plunger or paddle. The typical problem with this modulated force is that it gives rise to audible emissions that could be objectionable to people in the vicinity.

In some applications and appropriate PWM frequencies, current ripple (which causes force ripple or dither) can be useful in mitigating stiction[40] and hysteresis problems in the controlled actuator.

The maximum magnitude of the ripple current is important to the SCIS calculations discussed elsewhere in this document. One approach to determining the value is to use a simple simulation (for more details, see appendix *"A.3: Determining coil current settling time, steady state coil ripple current and steady state average value for a PWM waveform driving an inductive load"*).

PWB Layout Considerations

The PWB, for most applications, will be used to conduct heat out of the FDMS2380 so that it can operate without activating the FDMS2380 over temperature mechanism. Plated through holes may be exploited to help conduct heat, as well as conduct current, through the PWB to the back side of the board. In some cases, exotic techniques such as Direct Bond Copper (DBC), Insulated Metal Substrate (IMS) or other techniques will need to be employed to keep the FDMS2380 junction temperatures at acceptable levels.

All Gnd, Out and (to some extent, for flyback currents) V_{batt} traces (and, as needed, via's) need to handle the maximum currents expected for the application (see reference #16 for PWB design details). Although the over current trip point ($I_{out(trip)}$) can be as high as 30A, the FDMS2380 over current circuits react fast and disable the NMOS device within ~10μS, so these transient currents are of little concern.

Bypass capacitors for the V_{batt} pads are very important and must be physically close to the FDMS2380 pads (bypass capacitor requirements are discussed in the section below titled: "*Vbatt Bypass Capacitors*").

Consideration must be given to the surface mount attachment procedure as well as production inspection procedures.

V_{batt} Bypass Capacitors

Each FDMS2380 deployed in a system requires a high quality local power supply bypassing scheme. The purpose of the local bypassing scheme is to prevent fast, high voltage transients on the V_{batt} line from adversely affecting the operation of the FDMS2380.

Any scheme would include one or more *high quality* local bypass capacitors, between the V_{batt} and Ground pads and must be physically located as close as possible to the FDMS2380 terminals. The term *high quality* means that the bypass scheme's effective capacitance must have a low ESL and a low ESR.

More specifically, the FDMS2380 bypass scheme must reduce all V_{batt} transients with amplitudes passing through $V_{batt(ov)}$ (i.e., 27V to 32V) to have a rise time less than 2.2V/μS. System and board level requirements will constrain the selection of an appropriate scheme, but in many applications a single capacitor of at least 2.2μF with a rating of at least 60V in a 1210 package or smaller will usually be adequate.

In addition to local bypass capacitors, typically large value *board level* capacitors are needed to prevent medium-term V_{batt} transients from improperly effecting the operation of the overall board.

Typical Applications

A schematic diagram of a basic application is shown in Figure 42. There are many possible variations, but in the diagram shown there are two independent controllers, one for each solenoid.

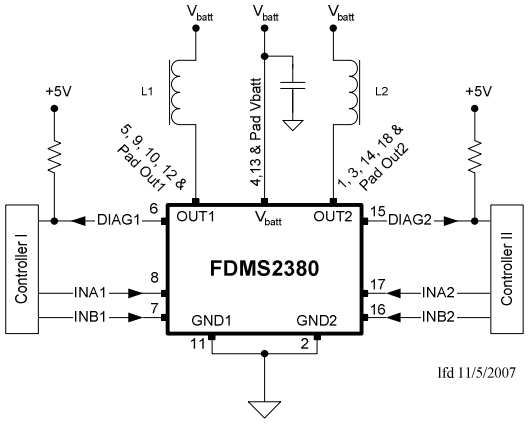

Figure 42: Basic Application Connections

The design process for a FDMS2380 based system might proceed as follows.

A system level analysis conducted for the application would result in a mechanical arrangement, force and timing profiles and ultimately, one or more candidates for each solenoid (it is likely that all solenoids in the system would have identical parameters). Given the parameters for each solenoid (e.g., inductance, coil resistance, etc.), and each force profile, a current profile could be derived for each solenoid. Given this information and each timing profile, a thermal analysis would be completed as described in previous sections. This iterative process would result in a set of operational parameters and solenoid parameters that would meet the overall system requirements as well as

[40] Stiction – Static Friction; for more details, see appendix *"A.6: Definition of Terms and Symbols"*

allow the FDMS2380 to operate within its capabilities. Given these results, a heat sinking scheme would be developed to confirm that the scheme can maintain FDMS2380 junction temperatures within limits. The feasibility and/or cost of the heat sinks may require another iteration of system parameter changes, thermal analysis and SCIS/UIS analysis for proper and safe system operation. Furthermore, a thermal analysis of the solenoid would be conducted and appropriate heat sinking, if needed, would be designed and implemented. During the analysis, the solenoid coil resistance temperature profile would be established and used in the analysis of the FDMS2380.

The next task is to design the PWB mounting for the FDMS2380. In addition to mounting the local power supply bypass capacitor in the best location, the trace widths for the Gnd, Out_1 and Out_2 signals need to be sized to carry the required maximum average current. It is important to note here that the two ground pads (2 and 11) are independent and must be tied together directly where the chip is mounted to the PWB.

Another aspect of the design process will be the development of the controller that interacts with the FDMS2380 logic signals. The lines for InA, InB and Diag (for each channel) must meet the logic level requirements and there must be a pull-up resistor on the open drain Diag FDMS2380 input. The hardware/software module that drives the InA and InB signals must be capable of meeting the needs of the PWM frequency and duty cycle as well as the timing profile demands of the application.

Added tasks for the controller are to monitor the FDMS2380 Diag signal, at the appropriate times, to capture signaled conditions (e.g., open load, flyback durations, etc.). For example, using the equation for time in clamp Equation 27 on page 37, the flyback time could be used to determine if there are faults in one or more of the solenoid windings.

Yet another task is to drive the FDMS2380 logic signals and interpret the results of special modes such as soft short.

The FDMS2380 Device Evaluation (DEV) Module and FDMS2380 Driver (DRV) Module

Evaluation items are available to assist customers considering applications for the FDMS2380. Currently, there are two Modules – *Device Evaluation (DEV) Module* and *Driver (DRV) Module*.

The DEV (Device Evaluation) Module is a very simple board that has one two-channel FDMS2380 device attached to a board with all signal pins brought out to convenient connection points. The board has a nominal amount of copper area dedicated to heat sinking. This board targets those that have a logic controller and want to evaluate the FDMS2380 in particular application sets.

The DRV (Driver) Module is the logic controller for the DEV Module. This Module has an on-board microprocessor that drives the FDMS2380 as a stand-alone device. The board has a simple pushbutton, LED and rotary selector as the user interface.

These Modules are available though the Fairchild Semiconductor's Sales organization and are supplied with user documentation.

Appendix

A.1: Example Estimating Coil Wire Length and D. C. Resistance Change over Temperature

Given the dimensions of a solenoid (e.g., see Figure 43), it is possible to estimate the length of wire needed to wind the coil (see reference #10) and thus the resistance of the coil at a particular temperature (see reference #10 et al). The Automotive temperature range will be used, which is: -40°C to +150°C.

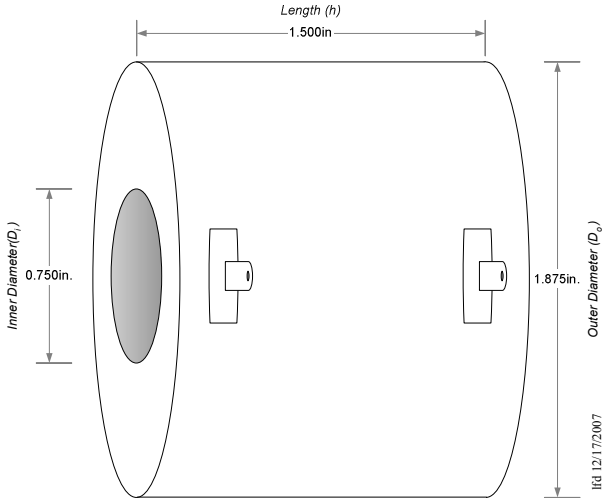

Figure 43: Example Solenoid Dimensions

The various dimensions of the solenoid are as follows:

Outer Diameter (D_o)	1.875	*in*
Inner Diameter (Di)	0.750	*in*
Delta ($D_o - D_i$)	1.125	*in*
Length (h)	1.500	*in*

Then the various dimensions of other parts of the solenoid construction (data from reference as shown):

Cover thickness (t_c)	0.005	*in*	(Reference #10, text page 164, "*Coil Covers*")
Tube Const: Wraps (N_w)	9		(Reference #10, table page 163)
Thickness (t_{wrap})	0.005	*in*	(Reference #10, table page 163)
Tube thickness (t_t)	0.045	*in*	$t_t=N_w*t_{wrap}$
Paper margin (t_p)	0.125	*in*	(Reference #10, table IV, page 165)

Next some basic calculations:

Net Winding Length (h_{nw})	1.250	*in*	$h_{nw}=h - 2*t_p$
Net Winding Depth (d_{nw})	0.513	*in*	$d_{nw}=(D_o-D_i)/2 - t_t - t_c$
Winding Net Area (S_w)	0.641	in^2	$S_w=h_{nw}*d_{nw}$
Perimeter of Mean Turn (P_m)	4.249	*in*	$P_m=\pi*(D_i + 2*t_t + d_{nw})$

The estimated number of turns for the coil can be calculated as $N = S_w*n_s$ (see reference #10, equation 9, page 171). The following is the basic data for various wire gauges (Data source for N_s, and R_c: Reference #10, Table V, page 169; R_i Table II page 158) and the calculation of the estimated number of turns (N):

Round Coil Wire Gage	N_s (turns/ sq in)	R_c (Ohms/ cu in)	R_i (Ohms/ 1,000 in)	N (Turns)	R_{coil} @°C +20.0
#28 wire	4,380	23.700	5.410	2,806	64.512
#24 wire	1,694	3.620	2.139	1,085	9.854
#22 wire	1,118	1.505	1.345	716	4.097
#20 wire	703	0.595	0.846	450	1.620
#18 wire	429	0.228	0.532	275	0.621

The resistance of the wire at 20°C is calculated as: $R = P_m * S_w * R_c$ (see reference #10, equation 11, page 171). With the resistance known at 20°C, the resistance can be determined at other temperatures as follows: $R_T = R_{20}[(-234-T)/-254]$ (from reference #10, et al). The following shows the estimated resistance at different temperatures and percent deviations:

Round Coil Wire Gage	Low R_{coil} @°C -40.0	Change from 20°C (%)	High R_{coil} @°C +150.0	Change from 20°C (%)	R Change over Range (%)
#28 wire	49.273	-23.6%	97.530	51.2%	97.9%
#24 wire	7.526	-23.6%	14.897	51.2%	97.9%
#22 wire	3.129	-23.6%	6.193	51.2%	97.9%
#20 wire	1.237	-23.6%	2.449	51.2%	97.9%
#18 wire	0.474	-23.6%	0.938	51.2%	97.9%

The results show that the solenoids coil resistance, using AWG20 wire, varies from 1.2Ω to 2.4Ω over the entire automotive temperature range which represents nearly a 98% variation. It is clear that the temperature effect must be taken into account for nearly all calculations involving solenoids that operate over the entire temperature range.

A.2: Derivation of Equations for Solenoid Force Calculations

The approach for the derivation of equations relating the force produced by a solenoid and the electrical drive parameters is to equate expressions for the energy in the magnetic field with the expressions for work done by the resultant mechanical motion. Once that basic force equation is determined, the equations for a particular mechanical arrangement can be derived for specific applications.

The work done by mechanical motion is calculated as force through a distance:

Equation 28: $$W_{mech} = \int f_{mech}(x)\, dx$$

This equation (or more precisely, the differential form) will be used as the right hand side of the equation to link with the electrical/magnetic left hand side and then the combination will be solved for the force.

A BH curve (Flux Density ***B*** Vs. Magnetic Field Intensity ***H***) for a particular solenoid is illustrated in Figure 44 and the graph shows that the characteristics are non-linear as well as that the coil is driven into saturation. The device must be operated in the linear area (within the rectangle as shown in Figure 44) and losses are ignored for this derivation.

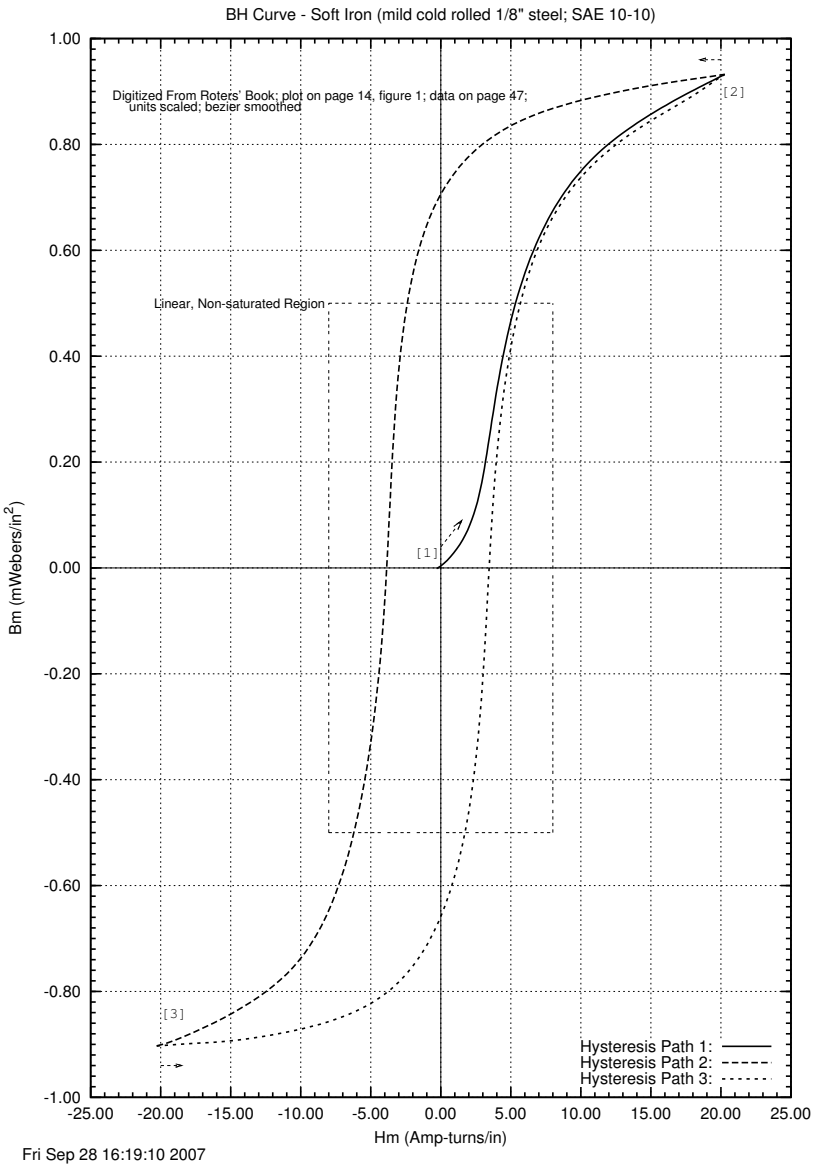

Figure 44: B-H Curve for a Solenoid

The energy in the magnetic field can be calculated using the B-H curve for the solenoid. One approach is to consider a dimensional analysis on the B and H quantities. One set of units for B (flux per unit area) is `webers/meter` (`1 weber = 1 Volt-Sec`) and one set for H (mmf per length) are `amp-turns/meter`, while energy can be measured in the units of `joules`.

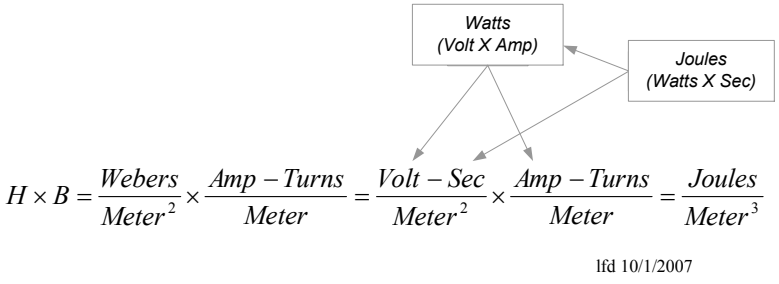

Figure 45: Dimensional Analysis of the Product B × H

The dimensional analysis details are illustrated in Figure 45 which shows that the product of B and H results in energy.

For ease in understanding in this case, the standard BH curve (Figure 44) was replotted in Figure 46 (H on Y axis, B on the X axis).

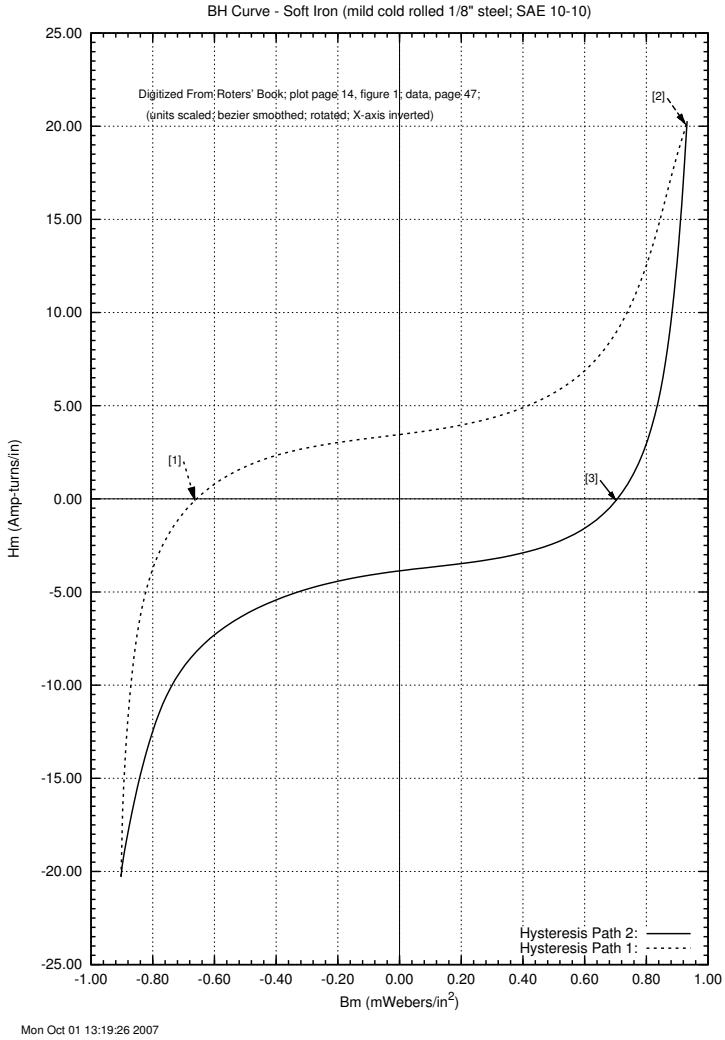

Figure 46: Replotted B-H Curve

The process begins (see Figure 46) with charging the magnetic field starting at the arrow marked "[1]" on the left of the graph near the B axis (H=0) and proceeds up to the arrow on the right marked "[2]" near the top of the graph. The area under this path represents the energy put into the magnetic field to build it up. Next the area under the path starting from the previous point (the arrow marked "[2]") proceeding to the last arrow (on the right near the B axis marked "[3]"; H=0 again) represents the energy removed from the collapsing magnetic field (these two area's are shown separately in Figure 47). That is, the entire path is [1] ➔ [2] ➔ [3], with [1] ➔ [2] being the magnetic build up and [2] ➔ [3] being the collapsing field.

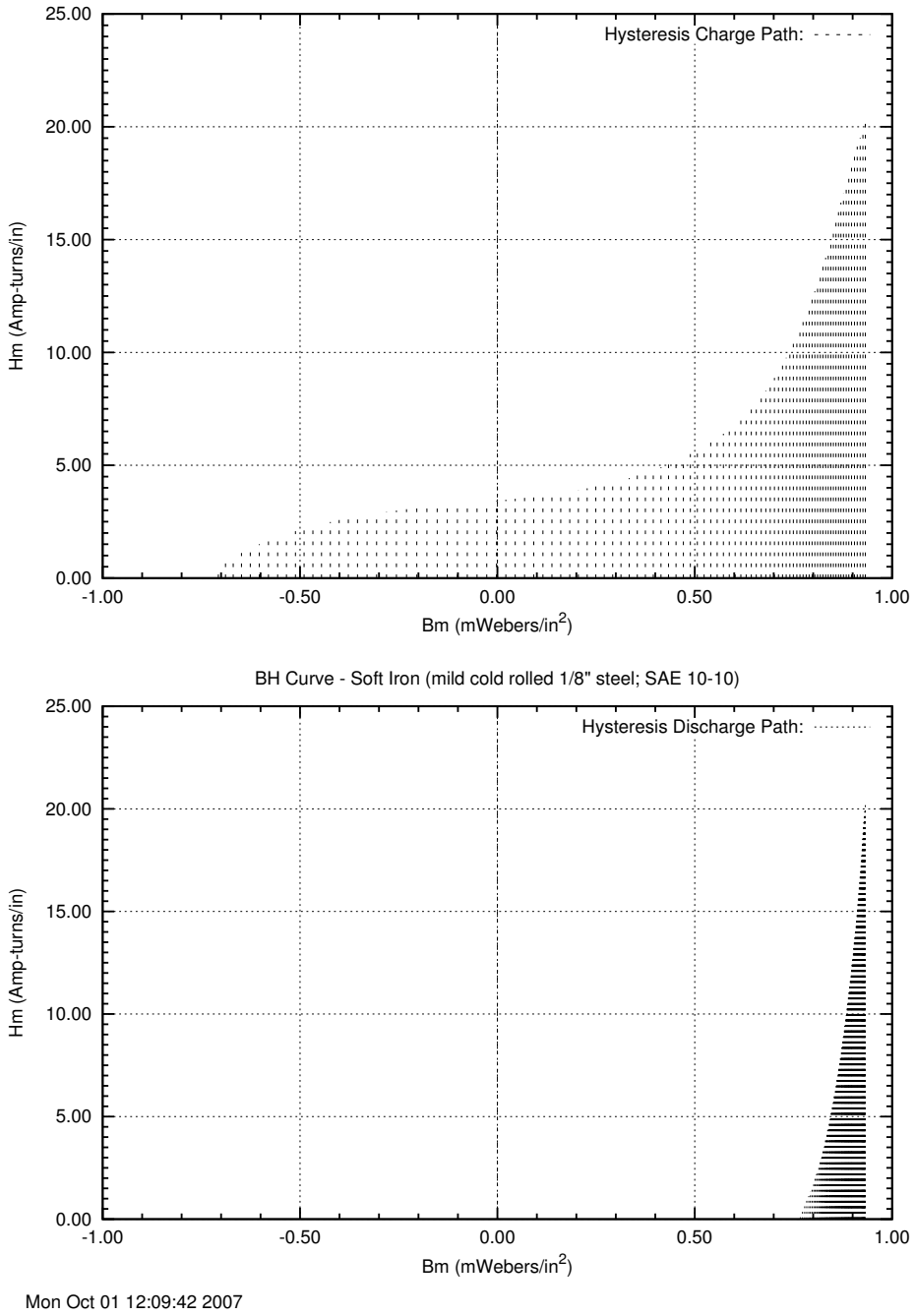

Figure 47: Area Under the Curve for Charging and Discharging a Magnetic Field

It is interesting to note, by inspection (see Figure 47), that the energy used to build the magnetic field is greater than the amount that is given up when it collapses. If the device is operated in the linear portion, then the area under the curve is the area under a right triangle or $\boxed{area = \frac{1}{2} \bullet Base \bullet Height}$ (the *base* is the value for the flux density ***B*** and the *height* is the value for the magnetic field intensity ***H***). Mathematically, this energy density is stated as:

$$\textbf{Equation 29: } w_{elec} = \frac{1}{2} BH$$

Given a cross sectional area A and a length L of the magnetic circuit, the total energy can be determined as:

$$\textbf{Equation 30: } w_{elec} = \frac{1}{2}BH = \frac{1}{2}B \bullet H \bullet A \bullet L = \frac{1}{2}(B \bullet A) \bullet (H \bullet L)$$

Knowing that $\Phi = BA$ and $\Im = HL$, the equation can be rewritten as:

$$\textbf{Equation 31: } w_{elec} = \frac{1}{2} \bullet \Phi \bullet \Im$$

Using Rowland's law $\Im = \Phi\Re$, substituting into the above equation and putting it in differential form, results in the following:

$$\textbf{Equation 32: } dw_{elec} = -\frac{1}{2}\Phi^2 d\Re$$

Using the differential form of Equation 28 for mechanical energy and then equating it to the energy above yields:

$$\textbf{Equation 33: } dw_{mech} = f(x)\,dx = dw_{elec} = -\frac{1}{2}\Phi^2 d\Re$$

Finally, solving for the force `f(x)` results in the equation:

$$\textbf{Equation 34: } f(x) = -\frac{1}{2}\Phi^2 \frac{d\Re}{dx}$$

This equation states that the force produced by a solenoid is proportional to the change in reluctance over a change in distance and the negative sign means that the direction in force is related to a decrease in reluctance of the magnetic circuit. Equation 34 can be used in specific mechanical arrangements to calculate resultant force (given, of course, the assumptions used to derive the equation – namely, no saturations and no losses).

A.3: Determining coil current settling time, steady state coil ripple current and steady state average value for a PWM waveform driving an inductive load

A closed form equation for the various operational parameters (e.g., transient settling time, steady state coil ripple current, etc.) could be derived. However, a more flexible approach would be to use some form of simulation that would include the specifics of the application. Specifics including the characteristics of the long interconnecting cables that drive the solenoid (e.g., cable capacitance, series resistance, inductance or a more complex distributed model), the solenoid itself (perhaps modeled as more than just a simple inductance and series resistance) and other aspects. This could be vital for demanding applications such as those that use closed loop position servo techniques or if the transient solution is most important for the application. In these cases, it may be better to use a PSpice simulation, a simulation written in a general purpose programming language such as Perl, C or others or even a custom spread sheet. The focus of the end application of the solenoids will dictate which approach to use.

One advantage of using a general purpose programming language to perform the simulation is that the results can also be analyzed and application specific results calculated and displayed (e.g., settling time etc.). Yet another advantage is that multiple runs can easily be performed to evaluate application parameter changes to show, for example, the effects of manufacturing tolerances, temperature changes, etc. A custom program for a simple solenoid application would center on using a physical model such as shown in Figure 6. The solenoid model would use a rising exponential (Equation 3 on page 4 or Equation 35 below) and a falling exponential (Equation 6 found on page 5 or Equation 39 below). The task would be the repeated application of these equations with the starting coil current amplitude of the next phase equal to the final value of the previous. The duration of the rising exponential is equal to the length of time of the PWM ON phase (PWM period times the duty cycle), while the falling exponential is the PWM OFF phase (PWM period times one minus the ON duty cycle). A simplified flowchart for such a simulation program is given in Figure 48.

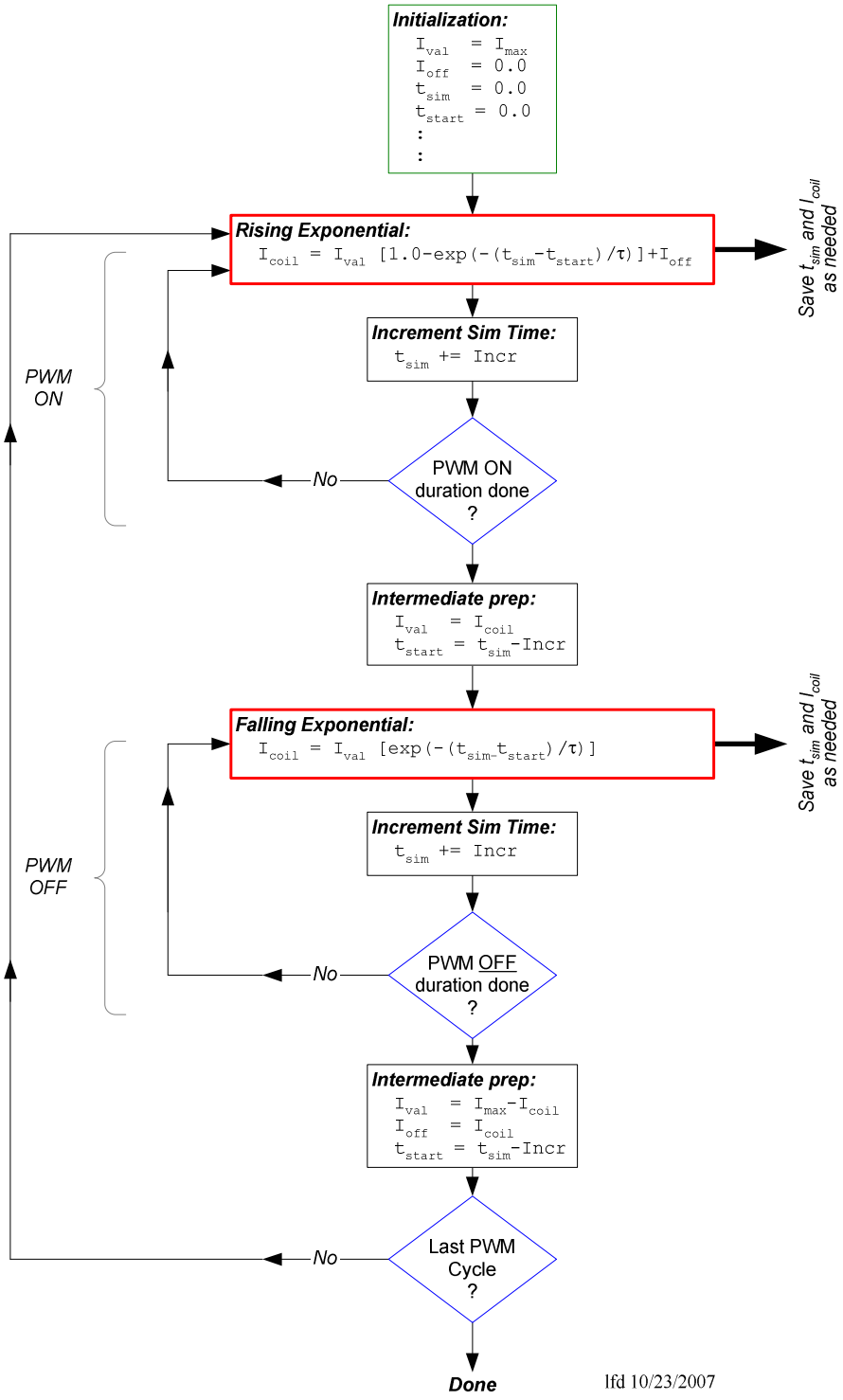

Figure 48: Simplified Flowchart for Numerical Simulation Program

The following is a short description of each of the variables used in the flowchart.

Variable	*Description*	*Variable*	*Description*
I_{coil}	Calculated coil current	t_{sim}	Running simulation time
I_{max}	Maximum coil current (typically, $I_{max} = V_{batt}/R_{coil}$)	Incr	Simulation step time increment
I_{val}	Maximum coil current amplitude for the exponential equation in a segment (e.g., PWM ON or PWM OFF segment)	t_{start}	Simulation time, set to the beginning of the calculation segment
I_{off}	Coil current offset for the exponential equation in a segment	τ	Circuit time constant (typically, $\tau = L_{coil}/R_{coil}$)

The main loop steps through simulated time, at some reasonable time increment, from zero through the number of PWM cycles to be simulated. There are two sub loops, one for the driven case (PWM ON), which lasts for the time duration of a single PWM ON pulse and one for the recirculation case (PWM OFF), with a time duration which is the same as that of a single PWM OFF pulse.

The t_{sim} and I_{coil} data that is generated can be evaluated during the run or saved to be evaluated by an independent program. Alternatively, the results can be plotted and the necessary parameters determined by visual inspection. The advantage of writing a program that evaluates the results is that a large number of runs can be made quickly with no manual intervention and thus a large variety of situation can be evaluated.

A.4: Derivation for the average value of a rising and falling exponential function

First, the rising exponential function is defined as follows:

$$\textbf{Equation 35:}\quad f(t) = A_{\max}\left(1 - e^{-t/\tau}\right)$$

The average value of a function over the time interval p → q is calculated as follows:

$$\textbf{Equation 36:}\quad f_{AVG} = \frac{1}{q-p}\int_p^q f(t)dt$$

Let $p=0$ and $q=t_{dur}$ (where t_{dur} is the duration of time to average and τ is the time constant as shown in Equation 35):

Substitute Equation 35 into Equation 36 and simplify:

$$f_{AVG} = \frac{1}{t_{dur}-0}\int_0^{t_{dur}} A_{\max}\left(1-e^{-t/\tau}\right)dt$$

$$f_{AVG} = \frac{A_{\max}}{t_{dur}}\left[\int_0^{t_{dur}} dt - \int_0^{t_{dur}} e^{-t/\tau}dt\right]$$

$$f_{AVG} = \frac{A_{\max}}{t_{dur}}\left[t\Big|_0^{t_{dur}} - \frac{1}{1/(-\tau)}e^{-t/\tau}\Big|_0^{t_{dur}}\right]$$

$$f_{AVG} = \frac{A_{\max}}{t_{dur}}\left[t_{dur} - \left(-\tau e^{-t_{dur}/\tau} - \left(-\tau e^{0}\right)\right)\right]$$

$$f_{AVG} = \frac{A_{\max}}{t_{dur}}\left[t_{dur} + \tau\left(e^{-t_{dur}/\tau} - 1\right)\right]$$

To simplify, use ρ (where ρ is the averaging duration in terms of the time constant τ) as follows:

Equation 37: $t_{dur} = \rho \times \tau \quad or \quad \rho = t_{dur} / \tau$

The final result:

Equation 38: $$\boxed{f_{AVG}(\rho) = A_{\max}\left[1 + \frac{1}{\rho}\left[e^{-\rho} - 1\right]\right]}$$

Second, the falling exponential function is defined as follows:

Equation 39: $f(t) = A_{\max}\ e^{-t/\tau}$

Again, let $p=0$ and $q=t_{dur}$ (where t_{dur} is the duration of time to average and τ is the time constant as shown in Equation 39):

Substitute Equation 39 into Equation 36 and simplify:

$$f_{AVG} = \frac{1}{t_{dur} - 0}\int_0^{t_{dur}} A_{\max} e^{-t/\tau} dt$$

$$f_{AVG} = \frac{A_{\max}}{t_{dur}}\left(-\tau\right)e^{-t/\tau}\Big|_0^{t_{dur}}$$

$$f_{AVG} = A_{\max}\frac{\tau}{t_{dur}}\left(-e^{-t_{dur}/\tau} + e^{0}\right)$$

Once more, to make things easier, use ρ (where ρ is the averaging duration in terms of the time constant τ) as follows:

Equation 40: $t_{dur} = \rho \times \tau \quad or \quad \rho = t_{dur} / \tau$

The end result:

Equation 41: $$\boxed{f_{AVG}(\rho) = \frac{A_{\max}}{\rho}\left[1 - e^{-\rho}\right]}$$

Under what conditions can a ramp function replace, to simplify calculations, a rising or falling exponential function?

If a less complicated average value calculation is needed, the simpler ramp function can be used instead of Equation 38 and Equation 41 (these involve the use of the complicated exponential function). However, this is only an approximation and so the following shows under what conditions the approximation is valid.

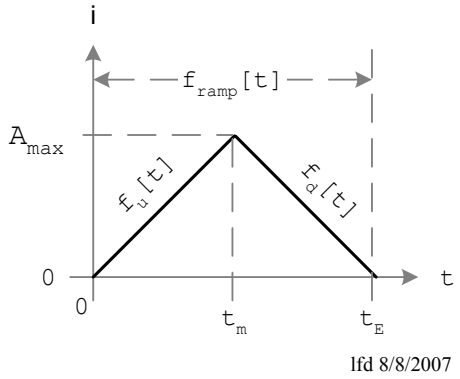

Figure 49: Ramp Function

Ramp function, $f_u[t]$, derivation, from time $t = 0$ to $t = t_m$: where: $f_u[0] = 0$; $f_u[t_m] = A_{max}$;

$f_u[t] = mt+b$; solve for m (slope) and b (intercept)

$@t=0$, $f_u[t] = 0$ then $0 = m*0+b \therefore b = 0$

$@t=t_m$, $f_u[t] = A_{max}$ then $A_{max} = m*t_m \therefore m = A_{max}/t_m$

So:

Equation 42: $\mathbf{f_u[t] = (A_{max}/t_m)*t \quad \forall\ t,\ 0 \le t \le t_m}$

Ramp function, $f_d[t]$, derivation, from time $t = t_m$ to $t = t_E$: where: $f_d[t_m] = A_{max}$; $f_d[t_E] = 0$;

$f_d[t] = mt+b$; solve for m (slope) and b (intercept)

$@t=t_m$, $f_d[t] = A_{max}$ then $A_{max} = m*t_m+b \therefore b = A_{max} - m*t_m$

$@t=t_E$, $f_d[t] = 0$ then $0 = m*t_E+b = m*t_E + A_{max} - m*t_m$ Solve for m

$\therefore m = -A_{max}/(t_E - t_m)$

So:

Equation 43: $\mathbf{f_d[t] = \{-A_{max}/(t_E-t_m)\}*(t-t_E) \quad \forall\ t,\ t_m \le t \le t_E}$

Case I: average value (use Equation 36 to determine the average value)

For the ramp function:

$$f_{u(avg)} = \frac{1}{t_m - 0}\int_0^{t_m} \frac{A_{\max}}{t_m} t\ dt = \frac{A_{\max}}{t_m^2}\frac{t^2}{2}\bigg|_0^{t_m} \quad \therefore\ f_{u(avg)} = \frac{A_{\max}}{2} \qquad \forall t,\quad 0 \le t \le t_m$$

$$f_{d(avg)} = \frac{1}{t_E - t_m}\int_{t_m}^{t_E} \frac{-A_{\max}}{t_E - t_m}(t - t_E)\ dt = \frac{-A_{\max}}{(t_E - t_m)^2}\left(\frac{t^2}{2}\bigg|_{t_m}^{t_E} - (t \bullet t_E)\bigg|_{t_m}^{t_E}\right)$$

$$= \frac{-A_{\max}}{(t_E - t_m)^2}\left(\frac{1}{2}\left(t_E^2 - t_m^2\right) - t_E\left(t_E - t_m\right)\right) = \frac{-A_{\max}}{(t_E - t_m)^2}\left(\frac{1}{2}\left(t_E + t_m\right)\left(t_E - t_m\right) - t_E\left(t_E - t_m\right)\right)$$

$$= \frac{-A_{\max}}{\left(t_E - t_m\right)}\left(\frac{1}{2}\left(t_E + t_m\right) - t_E\right) = \frac{-A_{\max}}{\left(t_E - t_m\right)}\left(\frac{1}{2}\left(t_m - t_E\right)\right) = \frac{A_{\max}}{2}$$

$$\therefore\ f_{d(avg)} = \frac{A_{\max}}{2} \qquad \forall t,\quad t_m \le t \le t_E$$

Equation 44: $$\therefore\ f_{u(avg)} = f_{d(avg)} = f_{ramp(avg)} = \frac{A_{\max}}{2} \qquad \forall t,\quad 0 \le t \le t_E$$

For the exponential rising and falling function (as shown in Figure 50):

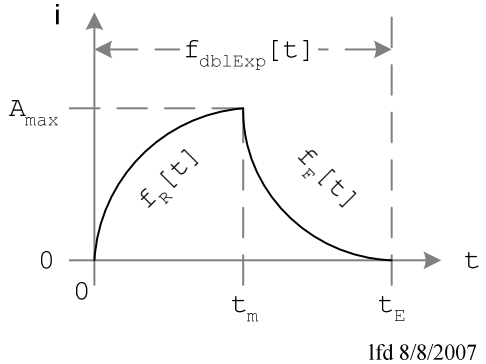

Figure 50: Rising and Falling Exponential Function

The equations are as follows:

- Rising exponential function: Equation 35 $f_{r}(t)$
  - Average value for rising exponential: Equation 38 $f_{r(avg)}(\rho)$
- Falling exponential function: Equation 39 $f_{f}(t)$
  - Average value for falling exponential: Equation 41 $f_{f(avg)}(\rho)$

The procedure is to equate $f_{u(avg)}=f_{r(avg)}[\rho]$ for the rising edge and then solve for ρ to find the value (or values) of ρ where the average of each are the same. Then, do the same calculation for the falling exponential and down ramp equations. Notice that the equation for the ramp function average is the same for the ramp up and the ramp down and it is independent of t for the given time range. Likewise, the rising and falling exponentials have the same equation for its average value.

Start with: $\frac{A_{\max}}{2} = A_{\max}\left[1+\frac{1}{\rho}\left(e^{-\rho}-1\right)\right]$ which simplifies to: $-\frac{1}{2} = \frac{e^{-\rho}-1}{\rho}$ and then plot the right hand side of the equation for a range of ρ values. The resultant plot is illustrated in Figure 51 and it shows ρ values that keep the right hand side within ±20% of -½ (the left hand side of the equation). The plot also shows that there is only one value where the equation is precisely satisfied.

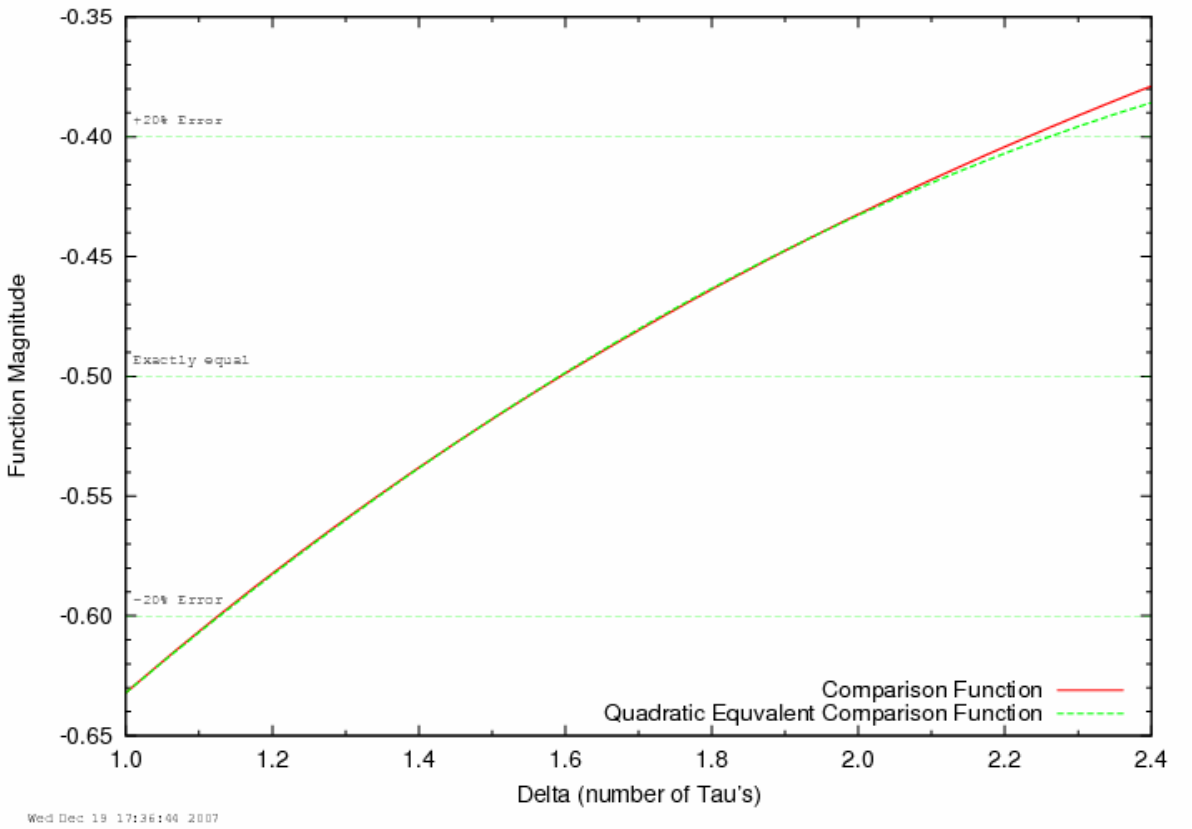

Figure 51: Plot of Ramp Vs. Exponential Comparison Function

Also shown in Figure 51 is a plot of a quadratic curve fit (i.e., $-\frac{1}{2}\pm 20\% = ax^2+bx+c$) which fits very well, when: $a = -0.058501$ $b = 0.374859$ and $c = -0.948479$. Note that using a Taylor series, even with a fifth order Taylor series expansion, did not work as well as a quadratic curve fit. Using the solution of the quadratic equation just mentioned (i.e., $\frac{-b \pm \sqrt{b^2-4ac}}{2a}$), the results are summarized as:

% *Error*	ρ *Range*
±10%	$1.346 \le \rho \le 1.883$
±20%	$1.128 \le \rho \le 2.261$

The equation for the falling edge of each function (see Equation 41 and Equation 44) is: $\frac{A_{\max}}{2} = \frac{A_{\max}}{\rho}\left[1-e^{-\rho}\right]$

and simplifies to: $-\frac{1}{2} = \frac{e^{-\rho}-1}{\rho}$, which is the same result as for the two rising exponential functions.

In summary, for the average value of a rising and falling ramp function to be within ±20% of a rising and falling exponential function (as in Equation 35 and Equation 39), the ρ parameter (which is the number of time constants) must be maintained between 1.128 and 2.261, otherwise, they are NOT equivalent.

This equivalency can be a useful simplification in calculating the energy dissipation during the excitation phase of a PWM cycle, for example. This is valid since the excitation duration is likely, for many duty cycle settings, to be on the order of 1.1 to 2.3 time constants in length.

A.5: Derivation of Time in Clamp Equation

Given the circuit as shown in Figure 41, and the following assumptions/simplifications:

- Changes in inductance due to force induced motion of the solenoid are ignored
- Clamp action is modeled as a constant voltage (V_{clamp}), which means the resulting equation is valid only up to the time when the circuit current goes to zero
- Results must be revised as T_j changes during flyback energy absorption
- Initial current is zero (i.e., $i(t=0)=0$)

The circuit equation, using the Kirchhoff's voltage law is:

Equation 45: $$-V_{clamp} = L_{coil}\frac{di(t)}{dt} + R_{coil}i(t)$$

The first step is to solve the ODE for i(t) and so, in general, for a first order non-homogeneous equation as:

$$\frac{di(t)}{dt} + f(t)i(t) = r(t)$$

The general solution[41] is:

$$i(t) = e^{-h}\left[\int e^{h} r dt + c\right] \quad Where: \quad h = \int f(t)dt \quad \text{and} \quad c \quad \text{is a constant of integration}$$

First rearrange Equation 45 into the standard form:

$$\frac{di(t)}{dt} + \frac{R_{coil}}{L_{coil}}i(t) = \frac{-V_{clamp}}{L_{coil}}$$

[41] See page 63 in reference #16

So that:

$$f(t) = \frac{R_{coil}}{L_{coil}} \quad and \quad r(t) = \frac{-V_{clamp}}{L_{coil}}$$

Substitute into the general solution:

$$h = \int f(t) = \int \frac{R_{coil}}{L_{coil}} dt = \frac{R_{coil}}{L_{coil}} t$$

$$i(t) = e^{-\frac{R_{coil}}{L_{coil}}t}\left[\int\left(e^{\frac{R_{coil}}{L_{coil}}t}\right)\left(-\frac{V_{clamp}}{L_{coil}}\right)dt + c\right]$$

$$i(t) = e^{-\frac{R_{coil}}{L_{coil}}t}\left[\left(\frac{L_{coil}}{R_{coil}}e^{\frac{R_{coil}}{L_{coil}}t}\right)\left(-\frac{V_{clamp}}{L_{coil}}\right) + c\right]$$

$$i(t) = ce^{-\frac{R_{coil}}{L_{coil}}t} - e^{-\frac{R_{coil}}{L_{coil}}t}\left(\frac{V_{clamp}}{R_{coil}}e^{\frac{R_{coil}}{L_{coil}}t}\right)$$

$$i(t) = ce^{-\frac{R_{coil}}{L_{coil}}t} - \frac{V_{clamp}}{R_{coil}}$$

To find the value of the constant of integration c, use one of the boundary conditions[42], namely $i(0) = I_{clamp} = \frac{V_{batt}}{R_{coil}}$

$$i(0) = I_{clamp} = \frac{V_{batt}}{R_{coil}} = ce^{-\frac{R_{coil}}{L_{coil}}0} - \frac{V_{clamp}}{R_{coil}} \quad solve\ for\ c$$

$$c = I_{clamp} + \frac{V_{clamp}}{R_{coil}}$$

The solution to the ODE is then:

Equation 46: $$i(t) = \left(I_{clamp} + \frac{V_{clamp}}{R_{coil}}\right)e^{-\frac{R_{coil}}{L_{coil}}t} - \frac{V_{clamp}}{R_{coil}}$$

Where: $I_{clamp} = \frac{V_{batt}}{R_{coil}}$ and $\tau = \frac{L_{coil}}{R_{coil}}$

[42] Notice that the maximum current is actually $I_{clamp}=V_{batt}/[R_{coil}+R_{ds(on)}]$, however, since $R_{coil} >> R_{ds(on)}$), $R_{ds(on)}$ can be ignored

Next, solve for the above equation for t_{clamp} when $i(t_{clamp})=0$:

$$i(t_{clamp}) = 0 = \left(I_{clamp} + \frac{V_{clamp}}{R_{coil}} \right) e^{-\frac{R_{coil}}{L_{coil}} t_{clamp}} - \frac{V_{clamp}}{R_{coil}}$$

$$\left(\frac{V_{clamp}}{R_{coil}} \right) \left(\frac{1}{I_{clamp} + \frac{V_{clamp}}{R_{coil}}} \right) = e^{-t_{clamp}/\tau}$$

$$\left(\frac{R_{coil}}{V_{clamp}} \right) \left(I_{clamp} + \frac{V_{clamp}}{R_{coil}} \right) = e^{t_{clamp}/\tau}$$

$$\log_e \left[e^{t_{clamp}/\tau} \right] = \log_e \left(\frac{I_{clamp}}{V_{clamp}} R_{coil} + 1 \right)$$

The final solution is:

Equation 47: $$t_{clamp} = \tau \log_e \left(1 + \frac{R_{coil}}{V_{clamp} / I_{clamp}} \right)$$

A.6: Definition of Terms and Symbols

Terms:

Term		*Description*
Alternator Load Dump Condition		This is a condition in an automobile (and standard automotive terminology) when the battery is disconnected while the alternator is turning and causes transients on the automobiles power distribution network. Load dump describes a fault condition whereby the alternator injects abnormal voltages on the V_{batt} line (80V to 100V for 300mS to 400mS). Circuits external to the FDMS2380 must be present to limit these transients from overstressing the FDMS2380.
Blanking Pulse		Before any protection (over voltage, over current, over temperature) diagnostic is signaled from the FDMS2380 a null time is forced on the Diagnostic output pin. This null time is accomplished by issuing a blanking pulse equal to the protection diagnostic in length (2µS to 10µS). This "blanking pulse" assures that if the diagnostic output was active for any reason, a fixed diagnostic off time will be implemented before the signaling of any protection fault. This assures the diagnostic protection pulse will be clearly defined at the output pin and avoids the possibility the system would miss a protection fault, as it would be attached and extended from a previous diagnostic signal without the blanking pulse timing.
CAE		Computer Aided Engineering
DBC		From *TheFreeDictionary* (http://encyclopedia.TheFreeDictionary.com/Direct+Bonded+Copper): Direct Bond Copper (DBC) substrates are commonly used in power modules, because of their very good thermal conductivity. They are composed of a ceramic tile (commonly alumina) with a

Term		*Description*
		sheet of copper bonded to one or both sides by a high-temperature oxidation process (the copper and substrate are heated to a carefully controlled temperature in an atmosphere of nitrogen containing about 30 ppm of oxygen; under these conditions, a copper-oxygen eutectic forms which bonds successfully both to copper and the oxides used as substrates). The top copper layer can be preformed prior to firing or chemically etched using printed circuit board technology to form an electrical circuit, while the bottom copper layer is usually kept plain. The substrate is attached to a heat spreader by soldering the bottom copper layer to it. Also see IMS
Clamp Circuit		The function of a clamp circuit is to limit the voltage across its terminals to a given maximum value. In the case of the FDMS2380, there are two clamp limit values of $V_{clamp(cl1)}$ and $V_{clamp(cl2)}$. To protect against load dump conditions, the NMOS transistor, in UIS mode, clamps the terminal value at $V_{clamp(cl1)}$ above V_{batt} (note that this is not a clamp circuit, but a characteristic of the discrete device) The $V_{clamp(cl2)}$ clamp circuit uses the PMOS transistor in an active mode to limit the connected solenoid coil to a value of $V_{clamp(cl2)}$ volts. That is, each of the two FDMS2380 out terminals is limited to $V_{clamp(cl2)}$ above the V_{batt} voltage when in flyback mode. Refer to the definitions for load dump, UIS and SCIS for more details.
Demagnetization		A solenoids operating mode whereby the intent is to dissipate the magnetic energy stored in the solenoid (demagnetize) so as to bring it to its resting position quickly. To perform this with a minimum of time, high voltages are generated (i.e., voltages higher than V_{batt}).
DISD		Dual Integrated Solenoid Driver or FDMS2380
DSO		Digital Sampling Oscilloscope
Eddy Currents Core Losses		Eddy current (also known as Foucault current) is an electrical phenomenon discovered by French physicist Léon Foucault in 1851. Eddy currents are associated with the circulating currents that exist in closed paths within the cores ferromagnetic material that cause unwanted heating. These circulating currents are caused by magnetic potential differences from the changing flux. Typically, thin laminations are used, instead of solid cores, to increase the resistance which reduces the losses. Note that the smaller the distance between adjoining laminations (i.e., the greater the number of laminations per unit area, perpendicular to the applied field), the greater is the reduction of eddy currents.
ESL		Effective Series inductance – Bypass Capacitor
ESR		Effective Series Resistance – Bypass Capacitor
FDMS2380 Operation Mode, Fast turn-off		This mode is used to quickly drain the magnetic energy stored in the solenoid.
FDMS2380 Operation Mode, Recirculation		This mode of FDMS2380 operation is used to maintain the magnetic energy in the solenoid during the PWM off period
Fast discharge		see Demagnetization
Fast turn-off		see Demagnetization
Flyback		see Demagnetization
IMS		From *TheFreeDictionary* (http://encyclopedia.TheFreeDictionary.com/Direct+Bonded+Copper): Insulated metal substrate (IMS) consists of a metal baseplate (aluminum is commonly used because of its low cost and density) covered by a thin layer of dielectric (usually an epoxy-based layer) and a layer of copper (35 µm to more than 200 µm thick).

Term		*Description*
		The FR-4-based dielectric is usually thin (about 100 µm) because it has poor thermal conductivity compared to the ceramics used in DBC substrates. Due to its structure, the IMS is a single-sided substrate, i.e., it can only accommodate components on the copper side. In most applications, the baseplate is attached to a heatsink to provide cooling, usually using thermal grease and screws. Some IMS substrates are available with a copper baseplate for better thermal performances. Compared to a classical printed circuit board, the IMS provides a better heat dissipation. It is one of the simplest way to provide efficient cooling to surface mount components Also see DBC
NDMOS		N-Channel Double-Diffused Metal-Oxide Semiconductor
ODE		Ordinary Differential Equation
PDMOS		P-Channel Double-Diffused Metal-Oxide Semiconductor
PQFN		Power Quad Flat No-lead package (aka Micro-lead frame or MLF™). The package was first developed circa 2003.
PWB		Printed Wiring Board (aka printed circuit board)
Rowland's Law		Named for American Physicist Henry Augustus Rowland (1848-1901) - Ohms law equivalent for magnetic circuits; Relates $\mathfrak{I}$, $\mathfrak{R}$ and Φ in a magnetic circuit Ohms Law — Rowland's Equivalent I (current) — Φ (flux) E (emf) — $\mathfrak{I}$ (mmf) R (resistance) — $\mathfrak{R}$ (reluctance) I = E/R — $\Phi = \mathfrak{I}/\mathfrak{R}$
SCIS		*Self Clamped Inductive Switching*; SCIS generally refers to a method for dissipating energy from a collapsing magnetic field of an inductive load such as a solenoid or other coil. Specifically, the active device (such as a power MOSFET, an IGBT, etc.) used to energize the coil is designed to also deactivate the coil. This is accomplished by dynamically limiting the voltage at its terminals (which are directly connected to the load) to a specific maximum voltage and thus absorbs energy from the collapsing magnetic field in the controlling devices active area. In this SCIS mode of operation, the devices gate is manipulated to control the current flow through the devices channel region. This clamping action removes the energy from the magnetic field at a speed determined principally by the magnitude of the clamp voltage. Absorbed energy is converted into heat concentrated in the active area of the device, which elevates its junction temperature. The power is dissipated through current flow in the channel region of the device which is controlled by the applied gate signal. A design analysis must be done to insure that the SCIS event or events do not exceed the devices junction temperature limits. It should be noted that it is sometimes the case that SCIS capability is required even if the load is not inductive. That is, there can be other elements in the system, beyond the load, that cause over voltage transients that must be absorbed by the active device. Also see UIS

Term		*Description*
Soft Short Detection		A FDMS2380 feature that detects shorts or near shorts between the output pin of each channel to ground See data sheet parameters $V_{out(ss)}$, T_{ss} and R_{ss}
SPICE		Simulation Program with Integrated Circuit Emphasis – family of circuit simulators derived from a 1970's UC Berkeley project
Stiction		"Two solid objects pressing against each other (but not sliding) will require some threshold of force parallel to the surface of contact in order to overcome static cohesion. Stiction is a threshold, not a continuous force."[43]
UIS		*Unclamped Inductive Switching*; UIS generally refers to a method for dissipating energy from an inductive load's collapsing magnetic field for devices such as solenoids or other coils. In this case, an active device (such as a power MOSFET, an IGBT, etc.) is used to not only energize the load, but also to de-energize it as well. The UIS method depends on the ability of the active device to dissipate the stored energy in its avalanche mode of operation. That is, for the UIS mode, the current flows through the PN junction that forms the devices body diode. The devices junction temperature elevates as it absorbs energy which is converted into heat concentrated in its active area. In the case of UIS, unlike SCIS, it is the breakdown of the body diode that absorbs the energy. That is, the power is dissipated at the PN junction that forms the body diode and the current flows to the metal of the source contact to the P body region. A design analysis must be done to insure that the UIS event or events do not exceed the devices junction temperature limits. It should be noted that it is sometimes the case that UIS capability is required even if the load is not inductive. That is, there can be other elements in the system, beyond the load, that cause over voltage transients that must be absorbed by the active device. Also see SCIS

Symbol definitions:

Symbol		*Description*
δ		An "ON" duty cycle (fraction from 0 to 1)
τ		A time constant (typically in units Seconds)
Φ		Magnetic flux (with units of Webers)
$\Im$		Magnetomotive Force (mmf with units of Ampere-Turns)
$\Re$		Magnetic reluctance (in units Ampere-Turns/Weber)
λ		A time duration (typically in units Seconds)
ρ		A ratio (dimensionless)

[43] For more details, see http://en.wikipedia.org/wiki/Stiction

Symbol		*Description*
η		Energy (typically in units Joules)
t		Time (typically in units Seconds)
T		Temperature (typically in units °C)
T_{amb}		Ambient temperature (typically in units °C)
T_j		Die junction temperature (typically in units °C), in the case the FDMS2380, it could be the PMOS, NMOS or Recirculation Diode die
R		Electrical resistance (typically in units Ω)
R_θ		Thermal resistance[44] (typically in units °C/W or K/W)
$R_{\theta jc}$		Thermal resistance[45] – junction to case (typically in units °C/W or K/W), in the case of the FDMS2380, there are two different values, one for the large pads and one for the small pad
$R_{\theta cs}$		Thermal resistance[46] –case to heat sink (typically in units °C/W or K/W)
$R_{\theta sa}$		Thermal resistance[47] – heat sink to ambient (typically in units °C/W or K/W)
V		Electrical voltage (typically in units Volts)
V_{batt}		Automobile battery (nominal value of 14.0 Volts)
I		Electrical current (typically in units Amperes)
P		Electrical Power (typically in units Watts)
f		Frequency (typically in units Hertz)
L		Electrical Inductance (typically in units Henrys)
C		Electrical Capacitance (typically in units Farads)
C_θ		Thermal Capacitance (typically in units Joules/°C)

[44] According to JESD51-12 ("*Guidelines for Reporting and Using Electronic Package Thermal Information*"): "Units of thermal resistance in °C/W are numerically equivalent to thermal resistance values in K/W."
[45] See footnote #44.
[46] See footnote #44.
[47] See footnote #44.

A.7: References

1. *"FDMS2380 Dual Integrated Solenoid Driver";* Fairchild Semiconductors Corporation; Data Sheet
2. "*MOSFET Basics*"; Fairchild Semiconductor Corporation ; Application Note AN9010
3. "*Power MOSFET Avalanche Guideline*"; Fairchild Semiconductor Corporation; Application Note AN9034
4. "*Single Pulse Unclamped Inductive Switching: A Rating System*", Fairchild Semiconductor Corporation; Application Note AN7514
5. "*A Combined Single Pulse and Repetitive UIS Rating System*", Fairchild Semiconductor Corporation; Application Note AN7515
6. "*Introduction to Power MOSFETs and their Applications*"; Fairchild Semiconductor Corporation; Application Note AN558
7. "*Design with MOSFET Load Switch*"; Fairchild Semiconductor Corporation; Application Note AN1030
8. "*Understanding Power MOSFETs*"; Fairchild Semiconductor Corporation; Application Note AN7500
9. "*Electrical Engineers' Handbook*"; Donald Christiansen; 4th edition 1996; ISBN 0-07-021077-2 (hc)
10. "*Electromagnetic Devices*"; Herbert C. Roters; 1st Edition 1941; ISBN: 0-47-173920-0
11. "*Electronic Transmission Controls*"; Edited by R. K. Jurgen; SAE (PT 79); 2000; ISBN: 0-7680-0631-7
12. "*An Analog Electronics Companion*"; Scott Hamilton; Cambridge University Press; 2003; ISBN: 0-521-79838-8
13. "*Inductance Calculations*"; Frederick Grover; Dover Phoenix; 2004 (1946); ISBN: 0-486-49577-9
14. "*Electromechanical Devices for Energy Conversion and Control Systems*"; Vincent Del Toro; Prentice-Hall; 1968;
15. "*Engineering Formulas*"; K. Gieck & R. Gieck; 8th Edition 2006; McGraw Hill; ISBN: 0-07-145774-7
16. "*Advanced Engineering Mathematics*"; Erwin Kreyszig; Second Edition 1967; John Wiley and Sons Inc.; (9th edition; 2005; ISBN 0471488852)
17. "*Generic Standard on Printed Board Design*"; IPC-2221A; May 2003; `www.ipc.org`
18. "*PCB Land Pattern Design and Surface Mount Guidelines for MLP Packages*"; Fairchild Semiconductor Corporation; Application Note AN-5067
19. "*Generic Requirements for Surface Mount Design and Land Pattern Standard*" IPC-7351 (supercedes IPC-SM-782); `www.IPC.org`
20. "*start: How to succeed the first time with ultra-small QFN packages*"; Duane Benson, Marketing Manager, Screaming Circuits; October 31, 2007; RF DesignLine, CMP Media LLC; URL: `http://www.rfDesignLine.com/202800634`
21. "Stress-Free Insulated Metal Substrate with Lowest Thermal Resistance for Large Area and High Power Modules"; AI Technology, Inc.; URL: `http://www.aitechnology.com/products/thermalinterface/thermclads/`
22. "Why DBC Substrates?"; Curamik Electronics; URL: `http://www.curamik.com/servlet/com.itmr.waw.servlet.FileViewer?sprachid=2&kid=160349&fid=261375&kdid=160108`

A.8: Acknowledgements

For their support and expert collaborations in creating this application note, many thanks from the author (Lawrence F. Durfee) are extended to:

- Jim Gillberg
- Jack Wojslawowicz
- Joe Nichols
- Ron Feiller
- Don Burton
- Alex Craig
- Mark Gluch

The author applauds the efforts of all the many people involved in the open software movement for the development and continued support of useful tools such as *GNU Plot*, *Engauge* and many others. These excellent Engineering tools played a prominent role in the development of this applications note.

A.9: Revisions

A. Rev A, released 04Feb2009

1. Corrected Equation 20 on page 25 to include the multiplication by the number of PWM cycles (N_{PWM}). Notice that the example (Step #5 on page 32) was correct and no change was needed.
2. Fixed the “Where:...” part of Equation 22 on page 25 which is the definition of t_{clamp}
3. Modified “Figure 33: FDMS2380 Forward-Biased Characteristics of the Internal Recirculation Diode” on page 26 to make it readable
4. Added t_{recirc} definition to “Figure 32: Data Needed for Calculating Power” on page 24
5. Made several miscellaneous changes for clarity and ease of understanding

PUBLICATION ORDERING INFORMATION

LITERATURE FULFILLMENT:
Literature Distribution Center for ON Semiconductor
19521 E. 32nd Pkwy, Aurora, Colorado 80011 USA
Phone: 303−675−2175 or 800−344−3860 Toll Free USA/Canada
Fax: 303−675−2176 or 800−344−3867 Toll Free USA/Canada
Email: orderlit@onsemi.com

N. American Technical Support: 800−282−9855 Toll Free USA/Canada
Europe, Middle East and Africa Technical Support:
Phone: 421 33 790 2910
Japan Customer Focus Center
Phone: 81−3−5817−1050

ON Semiconductor Website: **www.onsemi.com**

Order Literature: http://www.onsemi.com/orderlit

For additional information, please contact your local Sales Representative